Acta Pharmaceutica Sinica B 2025;15(6):3321−3337

Chinese Pharmaceutical Association
Institute of Materia Medica, Chinese Academy of Medical Sciences

Acta Pharmaceutica Sinica B

www.elsevier.com/locate/apsb
www.sciencedirect.com

ORIGINAL ARTICLE

Unveiling nonribosomal peptide synthetases from the ergot fungus *Claviceps purpurea* involved in the formation of diverse ergopeptines

Jing-Jing Chen, Ting Gong, Wei-Bo Wang, Tian-Jiao Chen, Jin-Ling Yang, Ping Zhu*

State Key Laboratory of Bioactive Substance and Function of Natural Medicines, NHC Key Laboratory of Biosynthesis of Natural Products, CAMS Key Laboratory of Enzyme and Biocatalysis of Natural Drugs, Institute of Materia Medica, Chinese Academy of Medical Sciences & Peking Union Medical College, Beijing 100050, China

Received 20 October 2024; received in revised form 15 January 2025; accepted 8 February 2025

KEY WORDS

Ergopeptine;
Biosynthetic mechanism;
Nonribosomal peptide (NRP) synthetase;
D-Lysergyl peptide synthetase A;
Heterologous expression;
NRP codes;
Chimeric enzymes;
Directed biosynthesis

Abstract Ergopeptines or their derivatives are widely used for treating neurodegenerative and cerebrovascular diseases. The nonribosomal peptide synthetase—D-lysergyl peptide synthetase A (LPSA) determines ergopeptine formation but the detailed mechanism remains to be elucidated. Here, we characterized two LPSAs from *Claviceps purpurea* Cp-1 strain through heterologous expression in *Aspergillus nidulans* feeding with D-lysergic acid. We proved that Cp-LPSA1 catalyzed the formation of ergocornine, α-ergocryptine, and β-ergocryptine, precisely controlled by the substrate specificity of its three modules. Cp-LPSA2 was initially inactive but could be restored to catalyze α-ergosine formation. Using this platform, we validated that P1-LPSA1 and P1-LPSA2 from the reported *C. purpurea* P1 strain catalyzed ergotamine and α-ergocryptine formation, respectively. Typically, the nonribosomal peptide codes implicated in every module of the LPSAs were defined and elucidated, in which certain key residues could play a switched role for substrate specificity and product interconversion. By constructing chimeric LPSAs through module assembly, the production of the desired ergopeptines was achieved. Notably, 1.46 mg/L of α-ergocryptine and 1.09 mg/L of ergotamine were produced respectively by mixed-culture of *C. paspali* No. 24 (fermentation supernatant) and the recombinants of *A. nidulans*. Our findings provide insights into the biosynthetic mechanism of ergopeptines and lay a foundation for directed ergopeptine biosynthesis.

*Corresponding author.
E-mail address: zhuping@imm.ac.cn (Ping Zhu).

Peer review under the responsibility of Chinese Pharmaceutical Association and Institute of Materia Medica, Chinese Academy of Medical Sciences.

https://doi.org/10.1016/j.apsb.2025.03.022

1. Introduction

Ergot alkaloids are important natural products produced by various ascomycete fungi, particularly those belonging to the Clavicipitaceae family, such as *Claviceps purpurea*[1,2]. *C. purpurea* grows on cereals and forms the sclerotia, commonly known as ergot[3,4]. The most active ergot alkaloids are ergopeptines, which are formed by amidating D-lysergic acid with a bicyclic tripeptide[5-7]. Ergopeptines exhibit structural diversity, featuring various amino acids in the first two positions of the bicyclic tripeptide, while the third position is consistently Pro[8-10]. Many natural ergopeptines or their semi-synthetic analogous possess valuable pharmacological activities and some have been developed into clinically important drugs[11-13]. Ergotamine and its derivative dihydroergotamine, which belong to 5-hydroxytryptamine receptor agonists, are commonly prescribed for treating acute migraines[14-16]. The derivatives of α-ergocryptine, including α-dihydroergocryptine (trade name: Vasobral) and bromocriptine, act as dopamine receptor agonists. α-Dihydroergocryptine is utilized for treating age-related neurological dysfunction and ischemic cerebrovascular disease[17] while bromocriptine is used for treating Parkinson's disease, acromegaly, and hyperprolactinemia[18]. Additionally, Hydergine (trade name), the mixture of α-dihydrogenated ergopeptines (α-dihydroergocryptine, β-dihydroergocryptine, dihydroergocristine, and dihydroergocornine), is used for treating dementia and age-related cognitive impairment (Supporting Information Fig. S1)[19].

The ergot alkaloid synthesis (EAS) gene cluster in *C. purpurea* has been identified (Fig. 1A), and the biosynthetic pathway of ergopeptines has been fundamentally elucidated[20-22]. According to previous studies, dimethylallyl pyrophosphate (DMAPP) and L-tryptophan are utilized to synthesize the intermediate D-lysergic acid (**1**) through a series of enzymatic reactions[23-26]. Subsequently, **1** is converted into ergopeptines by D-lysergyl peptide synthetase A (LPSA) and B (LPSB)[27,28], both belonging to the family of non-ribosomal peptide synthetases (NRPSs) and containing adenylation (A), thiolation (T) and condensation (C) domains[29,30]. Briefly, monomodular LPSB activates substrate **1**. Meanwhile, each module of the trimodular LPSA activates one of the three amino acids present in the bicyclic tripeptide. Activated **1** undergoes progressive elongation on LPSA through successive condensation reactions to form ergopeptams[31]. The ergopeptams are further oxidized by the dioxygenase EasH1, leading to the completion of the cyclol ring in the ergopeptines (Fig. 1B)[32]. Currently, at least 8 types of ergopeptines have been isolated from different *C. purpurea* strains. Each strain exhibits a distinct spectrum of ergopeptines (Fig. 1B and C). The structural diversity of ergopeptines is manifested in the bicyclic tripeptides which are assembled by the LPSAs.

Early studies deduced that the production of multiple ergopeptines by different *C. purpurea* strains might be related to the concentration of intracellular amino acid pools within these strains. *In vitro* experiments using D-dihydrolysergic acid and defined amino acids as the substrates showed that the LPSA and LPSB preparations from the *C. purpurea* D1 strain catalyzed the formation of several different dihydroergopeptams[28]. However, further study revealed that the EAS gene cluster in *C. purpurea* contains two LPSA members, including LPSA1 and LPSA2[20], which suggested that the previous *in vitro* experimental results might be attributed to the combined activities of both LPSA1 and LPSA2. In other words, the two LPSA members of each strain, together with LPSB, catalyzed the formation of all ergopeptines. Subsequent studies have revealed that most of the genes within the EAS gene cluster in different *C. purpurea* strains are highly conserved, but LPSA members exhibit significant variation[33,34]. This variability may contribute to the diversity of ergopeptine profiles among different *C. purpurea* strains. Up to now, only P1-LPSA1 from *C. purpurea* P1 strain, which is responsible for the biosynthesis of ergotamine, has been identified through gene deletion experiment, while the evidence for P1-LPSA2's function of this strain is still lacking[35]. In addition, it has been observed that certain strains, such as the Cp-1[36], Ecc93[20], and L-17[37], often produce more than two types of ergopeptines (Fig. 1C), suggesting that LPSA1 or LPSA2 in these *C. purpurea* strains must be involved in the biosynthesis of more than one ergopeptines. The detailed biosynthetic mechanism of ergopeptines is not yet fully understood. Therefore, it is necessary to carry out more systematic studies on LPSA members to elucidate the mechanism. Moreover, deeply studying the biosynthetic mechanisms of ergopeptines holds the promise of directed biosynthesis of specific ergopeptines to simplify the subsequent separation and preparation processes.

The *C. purpurea* Cp-1 strain, preserved in our lab, can produce multiple ergopeptines, including ergocornine (**2**), α-ergocryptine (**3**) and β-ergocryptine (**4**)[36]. This ergopeptine spectrum is different from the ergopeptine profiles produced by other reported *C. purpurea* strains. As a result, it becomes an ideal research material for investigating the biosynthetic mechanism of diverse ergopeptines. Firstly, the two new LPSA members (Cp-LPSA1 and Cp-LPSA2) from the Cp-1 strain were cloned and functionally characterized using *Aspergillus nidulans* A1145[38] as a heterologous expression host. Moreover, we utilized this platform to validate the substrate specificity of P1-LPSA1 and P1-LPSA2 from the aforementioned *C. purpurea* P1 strain through module swapping experiments. Most importantly, the non-ribosomal peptide codes (NRP codes) involved in every module of the LPSAs, which determine the substrate specificity, were defined and elucidated through site-specific mutagenesis, functional analysis, and molecular docking. On this basis, the functional modules of LPSAs with different substrate specificities were recombined to construct chimeric enzymes for the directed biosynthesis of specific ergopeptines.

2. Materials and methods

2.1. Strains, media, and growth conditions

Fungal strains used in this study are summarized in Supporting Information Table S1. *C. purpurea* Cp-1 strain and *C. paspali* No. 24 strain were cultured and fermented following the methods described previously[36,39].

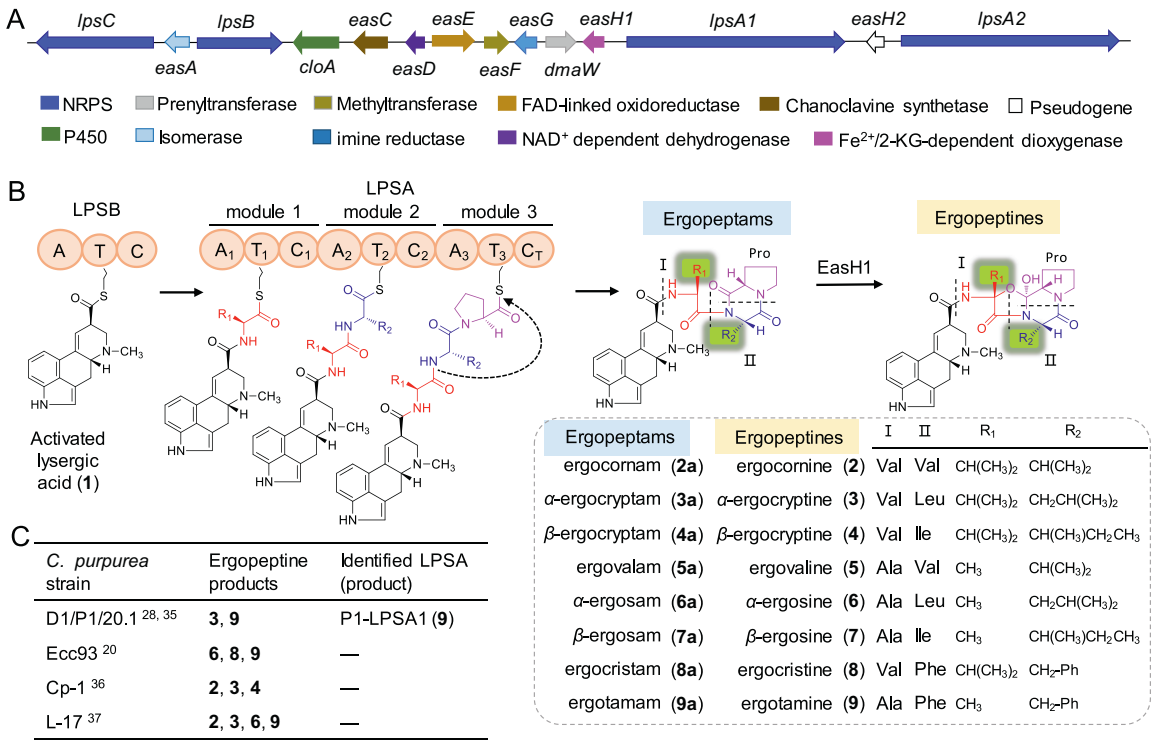

Figure 1 Biosynthesis of ergopeptines. (A) The reported gene cluster responsible for ergot alkaloid synthesis (EAS) in *C. purpurea*. (B) Monomodular LPSB activates D-lysergic acid (**1**), while each module of the trimodular LPSA activates one of the three amino acids present in the bicyclic tripeptide. The ergopeptine chain is progressively elongated on LPSA through successive condensations of activated **1** and the three amino acids, leading to the formation of ergopeptams. The ergopeptams are further oxidized by the dioxygenase EasH1, leading to the formation of the ergopeptines (Abbreviations: LPSA, D-lysergyl peptide synthetase A; LPSB, D-lysergyl peptide synthetase B; EasH1, a dioxygenase; A, adenylation domain; T, thiolation domain; C, condensation domain; C_T, terminal condensation domain. R_1 and R_2 represent different groups). (C) The types of ergopeptines produced by different *C. purpurea* strains.

Escherichia coli Trans1-T1 and BL21(DE3) cells were grown in LB medium (5 g/L yeast extract, 10 g/L tryptone, and 10 g/L NaCl). 50 mg/mL ampicillin was supplemented for the cultivation of recombinant *E. coli* strains.

Saccharomyces cerevisiae BJ5464-NpgA was used for *in vivo* yeast DNA recombination cloning. The cells were grown in the YPD medium (10 g/L yeast extract, 20 g/L peptone, and 20 g/L glucose). The SD medium lacking uracil was used for selection. *Aspergillus nidulans* A1145 was kindly provided by Prof. Yi Tang in the Department of Chemical and Biomolecular Engineering and Department of Chemistry and Biochemistry, University of California, California, United States. The strain was grown at 37 °C on GMM agar medium (1.0% glucose, 50 mL/L nitrate salt solution, 1 mL/L trace element solution) for sporulation and transformation with appropriate nutrition as required. The nitrate salt solution and trace element solution were described in previous references[40].

2.2. *Amplification of the functional genes of EAS gene cluster in C. purpurea Cp-1 strain*

C. purpurea Cp-1 strain was cultured and preserved on T25D agar medium as described previously[36]. For extraction of genomic DNA of *C. purpurea* Cp-1 strain, the mycelium was first grown on the T25D plate for 7 days, then inoculated in NL720 liquid medium (200 g/L sucrose, 15 g/L ammonium citrate, 0.25 g/L KH_2PO_4, 0.3 g/L $MgSO_4$, 1 mg/L $FeSO_4$, 30 mg/L $ZnSO_4$, at pH 5.2) and cultivated for 3 days, the mycelium was collected and ground in liquid nitrogen. The genomic DNA was extracted from the resulting cell powder. Polymerase chain reactions for cloning were performed using Q5 high-fidelity DNA polymerase (New England Biolabs, MA, USA) or FastPfu Fly DNA polymerase (TransGen Biotech, Beijing, China) as recommended by the manufacturer. The functional genes of the EAS gene cluster in the Cp-1 strain were amplified using the primers listed in Supporting Information Table S2. For obtaining the full sequences of Cp-*lpsA1* and *Cp-lpsA2* from the Cp-1 strain, the gene fragments were amplified using the primers Cp-lpsA1/A2-P1 and Cp-lpsA1/A2-P3, Cp-lpsA1/A2-P4 and Cp-lpsA1/A2-P6, Cp-lpsA1/A2-P2 and Cp-lpsA1/A2-P5, Cp-lpsA1/A2-S4F and Cp-lpsA1/A2-S4R, and Cp-lpsA1/A2-S5F and Cp-lpsA1/A2-S5R respectively. Then the chromosome walking technology was applied to obtain an unknown sequence at the 3′ terminal of *Cp-lpsA1* and *Cp-lpsA2* using the genome walking kit (Takara, Tokyo, Japan). Specifically, the three specific primers Cp-lpsA1/A2-SP1, Cp-lpsA1/A2-SP2, Cp-lpsA1/A2-SP3 with higher annealing temperature were designed, and thermal asymmetric PCR reactions were performed with the specific primers and degenerate primer (AP Primer, provided in the kit). Then the amplified fragment was cloned into the pEASY-simple blunt vector (TransGen) and sequenced. Finally, the segmented fragments were spliced together through overlapping regions to obtain the full sequences of *Cp-lpsA1* and *Cp-lpsA2*.

2.3. Heterologous expression of Cp-lpsA1, Cp-lpsA2, and recombinant Cp-lpsAs together with lpsB in A. nidulans

To construct plasmids for heterologous expression in *A. nidulans*, the yeast homologous recombination method was adopted. Briefly, the gene of *lpsB* carrying 200 bp terminator was amplified from the genomic DNA of *C. purpurea* Cp-1 strain using primers (lpsB-F-pANP and lpsB-R-pANP) containing 30 bp overlapping regions with the *A. nidulans* vectors. The gene of *lpsB* and PacI-digested pANP were co-transformed into *S. cerevisiae* BJ5464-NpgA using PEG/LiAc mediated transformation and selected on uracil-dropout semisynthetic agar medium. The plasmids from the correct yeast colonies were extracted using Zymoprep Yeast Miniprep Kit (Zymo Research, CA, USA) and transformed to *E. coli* Trans2-Blue (TransGen) for propagation and sequencing. The resulting recombinant plasmid was designated as pANP-lpsB. The genes of *Cp-lpsA1* and *Cp-lpsA2* were amplified in two segments using primers Cp-lpsA1/A2-1F and Cp-lpsA1/A2-AR, Cp-lpsA1/A2-BF and Cp-lpsA1/A2-3R. There were 100−300 bp homologous regions between the amplified fragments. The amplified DNA fragments of *Cp-lpsA1* and *Cp-lpsA2* were inserted into PacI-digested pANU, respectively, using the same procedures. The resulting recombinant plasmids were designated as pANU-Cp-lpsA1 and pANU-Cp-lpsA2, respectively.

A. nidulans A1145 was used as the recipient host. The protoplast preparation and transformation were performed as follows. Firstly, 1×10^9 spores of *A. nidulans* A1145 were inoculated and grown in 20 mL GMM liquid medium with 10 g/L yeast extract at 37 °C and 180 rpm for 5 h. The germinated spores were collected by centrifuging at 4 °C and 5500 rpm (Eppendorf, Hamburg, Germany) and washed twice with mycelium wash buffer (10 mmol/L sodium phosphate buffer, 0.6 mol/L $MgSO_4$, pH 7.0). Then 36 mg lysing enzymes from *Trichoderma harzianum* (Sigma−Aldrich, MO, USA) and 24 mg yatalase (Takara) were dissolved into 12 mL of osmotic buffer (10 mmol/L sodium phosphate buffer, 1.2 mol/L $MgSO_4$, pH 5.8) and added into the germlings. After digestion at 80 rpm and 30 °C for 6−8 h, the enzyme solution was poured into a 50-mL tube and 12 mL of trapping buffer (0.6 mol/L sorbitol, 0.1 mol/L Tris−HCl, pH 7.0) was gently added. The mixture was centrifuged at 4 °C and 3750 rpm for 15 min. The protoplasts at the middle layer were pipetted to a new tube, and added with an equal volume of STC buffer (10 mmol/L Tris−HCl, 1.2 mol/L sorbitol, 10 mmol/L $CaCl_2$, pH 7.5). The mixture was centrifuged at 4 °C and 5500 rpm for 15 min to obtain the protoplasts. The protoplasts were further resuspended with STC buffer and brought to a final concentration of 10^8 protoplasts. The constructed expression plasmid pANP-lpsB in combination with pANU-Cp-lpsA1 or pANU-Cp-lpsA2 was transformed into 100 μL of protoplasts and incubated on ice for 60 min, and then the 600 μL PEG solution (10 mmol/L Tris−HCl, 60% PEG4000, 50 mmol/L $CaCl_2$, pH 7.5) was added to the mixture, followed by additional incubation at room temperature for 20 min. Then the mixture was plated on GMM-sorbitol medium (GMM solid medium with 1.2 mol/L of sorbitol) and cultured at 37 °C for 2−3 days. The positive transformants were designated as An01 and An02, respectively. The empty plasmids pANU and pANP were introduced to *A. nidulans* to obtain the strain An-control, which was used as the control in this study. The recombinant expression strains were transferred to the GMM plates containing riboflavin and cultured for 3 days at 37 °C to obtain spores.

For cultivation and the products analysis of recombinant *A. nidulans* strains, approximately 1×10^7 fresh spores from positive transformants were used to inoculate 20 mL of CD-ST medium (GMM liquid medium containing 20 g/L starch without glucose) and cultured for 2 days at 25 °C and 180 rpm. 2 mg D-lysergic acid dissolved in DMSO was added to the broth with a final concentration of 0.1 mg/mL. The culture was shaken at 180 rpm for an additional 2 days at 25 °C and 180 rpm. The broth was adjusted to pH 8.0 and extracted with ethyl acetate. The extracts were evaporated under reduced pressure, resolved into methanol, and subjected to LC−MS analysis on a C18 column (5 μm, 2.1 mm × 100 mm), at the flow rate of 0.3 mL/min and the UV wavelength of 314 nm. Notably, the solvents used were (A) aqueous solution with 0.01 mol/L ammonium formate and (B) acetonitrile. The solvent gradient was % B, initial, 10%; 10 min, 15%; 13 min, 42%; 25 min, 42%; 30 min, 100%; 31 min, 10%; 36 min, 10%, with the run time of 36 min.

For investigating the function of Cp-LPSA2, the three functional modules of Cp-LPSA2 were respectively utilized to replace their counterparts in Cp-LPSA1. To construct the recombinant *Cp-lpsAs* with module swapping between *Cp-lpsA1* and *Cp-lpsA2*, the DNA fragments from each module of *Cp-lpsA1* and *Cp-lpsA2* were amplified, and these fragments and PacI-digested pANU backbone were mixed and transformed into yeast to generate plasmids pANU-Cp-lpsA2^{M1}Cp-lpsA1^{M2}Cp-lpsA1^{M3}, pANU-Cp-lpsA1^{M1}Cp-lpsA2^{M2}Cp-lpsA1^{M3}, pANU-Cp-lpsA1^{M1}Cp-lpsA1^{M2}Cp-lpsA2^{M3}, pANU-Cp-lpsA2^{M1}Cp-lpsA2^{M2}Cp-lpsA1^{M3}, and pANU-Cp-lpsA2^{M2}Cp-lpsA2^{M1}Cp-lpsA1^{M3}, respectively. Then these recombinant plasmids in combination with pANP-lpsB were transformed into the protoplasts of *A. nidulans,* resulting in the recombinant strains An03−An07 (Table S1), and the products of the recombinant strains were analyzed as mentioned above.

2.4. Constructions of mutant C. purpurea strain with Cp-lpsA1 or Cp-lpsA2 deletion

To generate the replacement fragments for *Cp-lpsA1* and *Cp-lpsA2*, the fusion PCR method was used as previously described[41]. Primers used to design constructs are listed in Table S2. Firstly, the DNA fragments at 5′ flank and 3′ flank of *Cp-lpsA1* and *Cp-lpsA2* were amplified using the primers Cp-lpsA1/A2-P1 and Cp-lpsA1/A2-P3, Cp-lpsA1/A2-P4 and Cp-lpsA1/A2-P6, respectively, from genomic DNA of the *C. purpurea* Cp-1 strain. As a selectable marker, the hph fragment was amplified from the plasmid pAN7-1 using the primers hph-F and hph-R. The three PCR products were combined and used as the template to generate the gene deletion fragments using the primers Cp-lpsA1/A2-P2 and Cp-lpsA1/A2-P5, which were used to transform Cp-1 strain. To prepare the protoplasts, the mycelium of the Cp-1 strain grown on the T25D plate was inoculated in NL720 liquid medium and cultivated at 220 rpm and 24 °C for 3 days, and then transferred to fresh NL720 medium again at 10% inoculum volume, and continued to culture for 24 h. The hyphae were harvested by centrifugation at 10,000 rpm and 4 °C for 10 min and washed with distilled H_2O twice. The mycelia were then transferred into a 100-mL flask with 5 mL of KCl (0.7 mol/L) containing 50 mg lywallzyme (Guangdong Microbial Culture Collection Center, Guangzhou, China). After shaking at 100 rpm and 25 °C for 1−2 h, the mixture was filtered through sterile cotton. The protoplasts were further pelleted by centrifugation for 10 min at 2200 rpm and resuspended with STC buffer (0.85 mol/L sorbitol, 50 mmol/L $CaCl_2$ in 0.1 mol/L Tris-HCI, pH 7.5) and brought to a final concentration of 10^8 protoplasts. *Cp-lpsA1* or *Cp-lpsA2* gene

deletion fragments (~10 μg) were mixed with 100 μL of the protoplasts, and the final volume was adjusted to 200 μL with STC. 50 μL of PEG solution (25% polyethylene glycol 4000, 50 mmol/L $CaCl_2$, 10 mmol/L Tris−HCl, pH 7.5) was added, and the mixture was incubated for 20 min on ice. Then, 2 mL STC buffer was added to the mixture and the mixture was further incubated at room temperature for 20 min. The process was stopped by dilution with 4 mL STC buffer. Finally, the suspension was added to 100 mL regeneration agar medium (10 g/L glucose, 4 g/L tryptone, 1 g/L yeast extract, 5 g/L beef extract, 2.5 g/L NaCl, 125 g/L sucrose, 5.1 $MgCl_2$, 2.78 g/L $CaCl_2$, 0.5 g/L K_2HPO_4, 25 mg/L sodium deoxycholate, 1.5 g/L agar, at pH 7.2) containing 1.2 mg/mL hygromycin B and spread on 5 Petri dishes. 7−10 days later, the transformants were transferred onto fresh T25D plates containing 1.5 mg/mL hygromycin B for isolation of genomic DNA to verify the gene deletion *via* PCR amplification. The diagnose primers were Cp-lpsA1/A2-P1 and hph-R, Cp-lpsA1/A2-P6 and hph-R, and Cp-lpsA1/A2-self-F and Cp-lpsA1/A2-self-R, respectively (Table S2). To screen the gene deletion homokaryons, a protoplasting process was performed due to the inability of the Cp-1 strain to sporulate. The potential gene-deleted *C. purpurea* strains and the parent Cp-1 strain were first cultivated in 50 mL seed medium at 240 rpm and 24 °C for 3 days in the dark. Then, 5 mL of this culture was transferred into the 80 mL fermentation medium and the cultivation was continued under the same condition for another 14 days. The ergopeptines were extracted and detected as previously described[36].

2.5. *Cp-lpsA1 and Cp-lpsA2 mRNA expression levels analysis of C. purpurea Cp-1 strain*

The mycelia of *C. purpurea* Cp-1 strain under the different fermentation stages were collected and lyophilized, and the total RNA was isolated using Trizol (Invitrogen, CA, USA) following the manufacturer's instructions. 100 mg of mycelia per sample was used as the starting material for the determination of total RNA. The reverse transcription polymerase chain reaction (RT-PCR) was carried out using TransScript All-in-One First-Strand cDNA Synthesis SuperMix (TransGen), and the cDNA was used for the real-time analysis. For real-time reverse transcription quantitative PCR (RT-qPCR), independent assays were conducted using the Ultra-SYBR One Step RT-qPCR kit (CWBIO, Beijing, China) with three biological replicates, and the expression levels were normalized to the mRNA level of tubulin. The $2^{-\Delta\Delta CT}$ method was used to determine the change in expression. The primers used for RT-qPCR are listed in Table S2.

2.6. *Expression, purification, and biochemical characterization of A domains of Cp-LPSA1 and Cp-LPSA2*

The boundaries of A domains in Cp-LPSA1 and Cp-LPSA2 were predicted by CD-search in NCBI, and then the intron-free sequences of A domains were amplified by using the cDNA of *C. purpurea* Cp-1 strain as template and the primers Cp-lpsA1/$A2^{Ade1}$-F and Cp-lpsA1/$A2^{Ade1}$-R, Cp-lpsA1/$A2^{Ade2}$-F and Cp-lpsA1/$A2^{Ade2}$-R, respectively (Table S2). The PCR products were digested with EcoR I and Xho I and ligated into pCold TF digested with the same restriction enzymes to generate the plasmids pCold TF-Cp-lpsA1^{Ade1}, pCold TF-Cp-lpsA1^{Ade2}, pCold TF-Cp-lpsA2^{Ade1} and pCold TF-Cp-lpsA2^{Ade2}, respectively (Table S1). All the correct constructs were verified by DNA sequencing. These constructed plasmids were transformed to chemically competent *E. coli* BL21 (DE3) by heat shock and grown overnight at 37 °C on an LB agar plate supplemented with 50 μg/mL ampicillin. For protein induction and purification, the single colony was inoculated into LB media overnight as seed culture at 37 °C. After inoculated into fresh LB medium at 1% (*v*/*v*), cells were grown at 37 °C and 220 rpm supplemented with the 50 μg/mL ampicillin to a final OD_{600} around 0.6. The culture was quickly cooled to 15 °C in ice water, and let stand for 30 min. Then the 0.1 mmol/L IPTG was added to induce protein expression and the cells were incubated with shaking at 15 °C for an additional 24 h. Then, the cells were harvested by centrifugation for 10 min at 10,000×g, and washed and resuspended in buffer A (150 mmol/L NaCl, 20 mmol/L Tris−HCl, pH 8.0). The cells were lysed by sonication (60 × 5 s cycles), and the cellular debris was removed by centrifugation for 30 min at 12,000×*g* two times. After filtration through a 0.45 μm filter, the supernatant was subjected to a 5-mL HisTrap HP column (GE Pharmacia, NY, USA) using an AKTA purifier, and then eluted with gradient from 0 to 100% buffer B (150 mmol/L NaCl, 300 mmol/L imidazole, 20 mmol/L Tris−HCl, pH 8.0) for 20 column volumes at a flow rate of 2 mL/min. Then the elution was concentrated and further applied to a HiTrap desalting column (GE Pharmacia) washed with storage buffer (50 mmol/L Tris−HCl, 50 mmol/L NaCl, 5% glycerol, 0.5 mmol/L EDTA, pH 8.0). The purified protein was confirmed by SDS-PAGE and stored at −80 °C with 5% glycerol. The activities of the A domains of Cp-LPSA1 and Cp-LPSA2 on 19 types of standard essential amino acids as substrates were measured by monitoring the release of PPi at 360 nm using the EnzChek pyrophosphate assay kit according to the manufacturer's recommendation (Life Technology, NJ, USA). In detail, 10 μL of suitably diluted A domain proteins was added to each 100 μL reaction system, which contained 5 μL 20 × reaction buffer, 20 μL MESG, 1 μL of PNP (1 U), 5 mmol/L ATP, 5 mmol/L substrate. Reactions were carried out at 30 °C on a multimode plate reader Enspire (PerkinElmer, MO, USA) using a 96-well plate, measured by monitoring PPi release at 360 nm continuously for 30 min. The standard curve of the pyrophosphate assay was generated using standard pyrophosphate. Reactions for each A domain protein were conducted in triplicate with boiled A domain proteins as control.

2.7. *Functional characterization of P1-LPSA1 and P1-LPSA2 through heterologous expression*

For examining the functions of the P1-LPSA1 and P1-LPSA2 from *C. purpurea* P1 strain, the *P1-lpsA1* and *P1-lpsA2* genes were synthesized by BGI (Beijing, China) based on the sequences registered in GenBank. The 3′ end of *P1-lpsA2* was found to have additional 16 bases of discontinuous insertions and one base of deletion compared to the other reported *lpsAs*, which may potentially cause the downstream mutation, thus a modified version of *P1-lpsA2* (*P1-lpsA2**) was also synthesized, in which the inserted or missing bases are corrected. Each of the synthesized *P1-lpsA1*, *P1-lpsA2*, and *P1-lpsA2** was mixed with PacI-digested pANU and transformed into yeast to generate plasmids pANU-*P1-lpsA1*, pANU-*P1-lpsA2* and pANU-*P1-lpsA2**, respectively. Then the recombinant plasmids in combination with pANP-lpsB were transformed into the protoplasts of *A. nidulans,* resulting in the recombinant strains An12−An14 (Table S1). To construct chimeric enzymes containing functional modules of LPSAs from the Cp-1 strain and the P1 strain, the DNA fragments of different LPSAs modules were amplified, and the recombinant

plasmids were constructed, named pANU-P1-lpsA1^{M1}Cp-lpsA2^{M2}Cp-lpsA1^{M3}, pANU-P1-lpsA1$^{M1}{}_{m}$Cp-lpsA2^{M2}Cp-lpsA1^{M3}(where P1-lpsA1$^{M1}{}_{m}$ includes the restored missing 767 bp at the 5′ end using the homologous sequence of *Cp-lpsA2*), pANU-P1-lpsA2^{M1}Cp-lpsA2^{M2}Cp-lpsA1^{M3}, pANU-Cp-lpsA1^{M1}1-lpsA1^{M2}Cp-lpsA1^{M3}, pANU-Cp-lpsA2^{M1}P1-lpsA1^{M2}Cp-lpsA1^{M3}, pANU-Cp-lpsA1^{M1}P1-lpsA2^{M2}Cp-lpsA1^{M3}, pANU-Cp-lpsA2^{M1}P1-lpsA2^{M2}Cp-lpsA1^{M3}, pANU-Cp-lpsA1^{M1}Cp-lpsA2^{M2}P1-lpsA1^{M3}, pANU-Cp-lpsA1^{M1}Cp-lpsA2^{M2}P1-lpsA1$^{M3\#}$ (where P1-lpsA1$^{M3\#}$ includes the restored missing 363 bp at the 3′ end using the homologous sequence of *Cp-lpsA1*), pANU-Cp-lpsA2^{M1}Cp-lpsA2^{M2}P1-lpsA2^{M3}*(where P1-lpsA2^{M3}* refers to the correction of the inserted or missing bases in its module 3), pANU-Cp-lpsA1^{M1}Cp-lpsA2^{M2}P1-lpsA2^{M3}*, and pANU-Cp-lpsA1^{M1}Cp-lpsA2^{M2}P1-lpsA2$^{M3\#}$ (where P1-lpsA1$^{M3\#}$ refers to the compensation for the missing 118 bp at the 3′ end using the homologous sequence based on *P1-lpsA2^{M3}**), respectively (Table S1). Then the recombinant plasmids in combination with pANP-lpsB were transformed into the protoplasts of *A. nidulans,* resulting in the generation of recombinant strains An15−An21 and An24−An28 (Table S1). The products of the recombinant strains were analyzed as previously mentioned.

2.8. Constructions of ergopeptine-producing recombinant strains

The DNA fragment of *easH1* was amplified from the genomic DNA of Cp-1 strain using primers (easH1-F and easH1-R) and cloned into pANR to generate pANR-easH1. Then the pANR-easH1 was introduced into the corresponding ergopeptam-producing strains, resulting in the generation of recombinant strains An08−An11, and An22−An23 (Table S1). The products of the recombinant strains were analyzed as previously mentioned. To isolate compounds **3**, **6**, **8**, and **9**, the fresh spores from the recombinant strains An09, An11, An22, and An23 were respectively used to inoculate CD-ST liquid medium, and cultured for 2 days (25 °C, 180 rpm). D-lysergic acid dissolved in DMSO was added to the broth. The culture was sequentially shaken at 180 rpm for an additional 2 days (25 °C, 180 rpm). The products were extracted as mentioned previously. The targeted compound was further isolated and purified using semi-preparative HPLC. The isolated products were dissolved in DMSO-d_6 or $CDCl_3$. NMR spectra of the samples were recorded at room temperature on an INOVA 600 NMR spectrometer (Varian, CA, USA) to obtain ^{1}H NMR, ^{13}C NMR, HSQC, and HMBC spectra.

2.9. Combinatorial and single-directed mutagenesis of Cp-LPSA1

According to the method mentioned above, the recombinant plasmids containing multiple or single point mutations were constructed, named as pANU-Cp-lpsA1^{M1}Cp-lpsA1$^{M2-penta}$Cp-lpsA1^{M3}, pANU-Cp-lpsA1^{M1}P1-lpsA1$^{M2-penta}$Cp-lpsA1^{M3}, pANU-Cp-lpsA1-A196V, pANU-Cp-lpsA1-V254M, pANU-Cp-lpsA1-G256A, pANU-Cp-lpsA1-I285V, pANU-Cp-lpsA1-I286G, and pANU-Cp-lpsA1-I286A, respectively. The recombinant plasmids in combination with pANP-lpsB were transformed into the protoplasts of *A. nidulans,* resulting in the generation of recombinant strains An29−An36 (Table S1). The products of the recombinant strains were analyzed by LC−MS as previously mentioned.

2.10. Molecular docking using AutoDock Vina tools

The three-dimensional structures of the second A domain in Cp-LPSA1 and P1-LPSA1 (referred as Cp-LPSA1^{Ade2} and P1-LPSA1^{Ade2}) were predicted from Swiss model http://swissmodel.expasy.org/)[42] using the available structure of A domain of gramicidin synthetase 1 (Protein Data Bank code 11AMU), which has 28% sequence identity and 34% sequence similarity to Cp1-LPSA1^{Ade2}, and 29% sequence identity and 34% sequence similarity to P1-LPSA1^{Ade2} as a template. The predicted 3D structure and substrate aminoacyl-AMP were selected for the docking experiments with AutoDockTools Proteins, preprocessed by deleting the water molecules, adding hydrogen, and computing Gasteiger charges. The ligands were preprocessed by adding polar hydrogen and detecting roots. The grid size was set to cover the ten key positions that are relevant for substrate specificity which are collectively referred to as the nonribosomal code. The conformations that the ligand bound to the cavity inside the protein and had the lowest binding free energies were selected as the optimal docking poses. PyMOL was used to visualize molecular docking results.

2.11. Mixed-culture of C. paspali and recombinant A. nidulans for the production of ergopeptines

The *C. paspali* No. 24 strain was first cultured for 10 days as previously reported[39]. On the 8th day of *C. paspali* No. 24 cultivation, the recombinant *A. nidulans* was cultured in a liquid CD-ST medium as mentioned above. Subsequently, *C. paspali* No. 24 and recombinant *A. nidulans* were co-cultivated for 2 days at different ratios of inoculation volumes, or different volumes of *C. paspali* No. 24 fermentation supernatant were added to the culture of recombinant *A. nidulans*, followed by continued cultivation for another 2 days. The production of specific ergopeptines was analyzed as previously described[36].

3. Results

3.1. Gene cloning and sequence analysis of Cp-lpsA1 and Cp-lpsA2 in C. purpurea Cp-1 strain

Based on the published sequence information of the EAS gene cluster of *C. purpurea* 20.1 strain available on NCBI (GenBank accession no. JN186799.1), all the genes within the EAS gene cluster of *C. purpurea* Cp-1 strain were amplified. Specifically, the full sequences of *Cp-lpsA1* (GenBank accession no. PQ097018.1) and *Cp-lpsA2* (GenBank accession no. PQ097019.1), each with a length of 10.9 kb, were obtained through segmented amplification combined with chromosome walking technology. Conserved domain search analysis confirmed that both Cp-LPSA1 and Cp-LPSA2 in the Cp-1 strain belonged to trimodular NRPS, with each module containing the A, T, and C domains. Most genes of the EAS gene cluster between the Cp-1 and 20.1 strains exhibited 97%−100% sequence identity (Supporting Information Table S3). However, both *Cp-lpsA1* and *Cp-lpsA2* only maintained 84.6%−94.8% amino acid sequence identity with those from other *C. purpurea* strains (Supporting Information Table S4), confirming the previous opinion that the sequence heterogeneity in *lpsAs* resulted in different ergopeptines profiles among *C. purpurea* strains[20]. Furthermore, the amino acid sequence identity between *Cp-lpsA1* and *Cp-lpsA2* was only 86.7%, suggesting that they may

be responsible for synthesizing different ergopeptines in the Cp-1 strain.

*3.2. Cp-LPSA1 catalyzes the formation of ergocornine (**2**), α-ergocryptine (**3**), and β-ergocryptine (**4**)*

Due to its clean genetic background, robust native gene-splicing system, and superior eukaryotic protein expression capability[43-45], the filamentous fungus *A. nidulans* A1145 was selected as a heterologous expression host to investigate the function of Cp-LPSAs. These advantages ensure accurate gene splicing and efficient expression of the giant fungal LPSAs. Consequently, either *Cp-lpsA1* or *Cp-lpsA2*, along with *lpsB*, was introduced into the *A. nidulans* A1145 host to generate strains An01 and An02, respectively. The recombinant strains were cultured by feeding D-lysergic acid as one of the substrates, and the resulting products were analyzed by liquid chromatography-mass spectrometry (LC−MS). Co-expression of *Cp-lpsA1* and *lpsB* in *A. nidulans* host led to the formation of **2a** (the $[M + H]^+$ ion at *m/z* 546), **3a** (the $[M + H]^+$ ion at *m/z* 560), and **4a** (the $[M + H]^+$ ion at *m/z* 560) (Fig. 2Aii and Supporting Information Fig. S2). The oxygenase EasH1 was added to strain An01 to generate strain An08, where **2a** and **3a** were further converted into ergocornine (**2**) and α-ergocryptine (**3**), respectively (with **4** potentially being too low to be detected) (Fig. 3A and Bii). The structures of these products were identified through MS detection and NMR analysis (Supporting Information Figs. S2, S19 and S20, Table S6). Thus, **2a** and **3a** were identified as ergocornam and α-ergocryptam, respectively. The identification of **3a** was further supported by the product analysis of the recombinant strain An09, which produced only **3** (Fig. 3A and Biii). Consequently, **4a** was inferred to be β-ergocryptam. These ergopeptams were the precursors of **2**, **3**, and **4**, which were the primary products of the *C. purpurea* Cp-1 strain (Fig. 2Aix). To our surprise, no ergopeptams were produced when *Cp-lpsA2* and *lpsB* were co-expressed in the *A. nidulans* host (Fig. 2Aiii). The reason was later confirmed to be the inactivation of module 3 of Cp-LPSA2 (see below).

Meanwhile, we also tried to delete the *Cp-lpsA1* and *Cp-lpsA2* genes from the *C. purpurea* Cp-1 strain, respectively. Due to the non-sporulation of *C. purpurea* under laboratory conditions, the gene-deleted mutants had to be selected by the protoplasting process. However, it is challenging to acquire a complete gene knockout because of the multinucleate characteristic of the protoplasts. After screening hundreds of single colonies, the homokaryotic *Cp-lpsA2* deletion mutant (*ΔCp-lpsA2*) was obtained, while the *Cp-lpsA1* knockout mutant (*ΔCp-lpsA1*$_{hetero}$) remained heterokaryotic, meaning that the *Cp-lpsA1* gene was deleted in

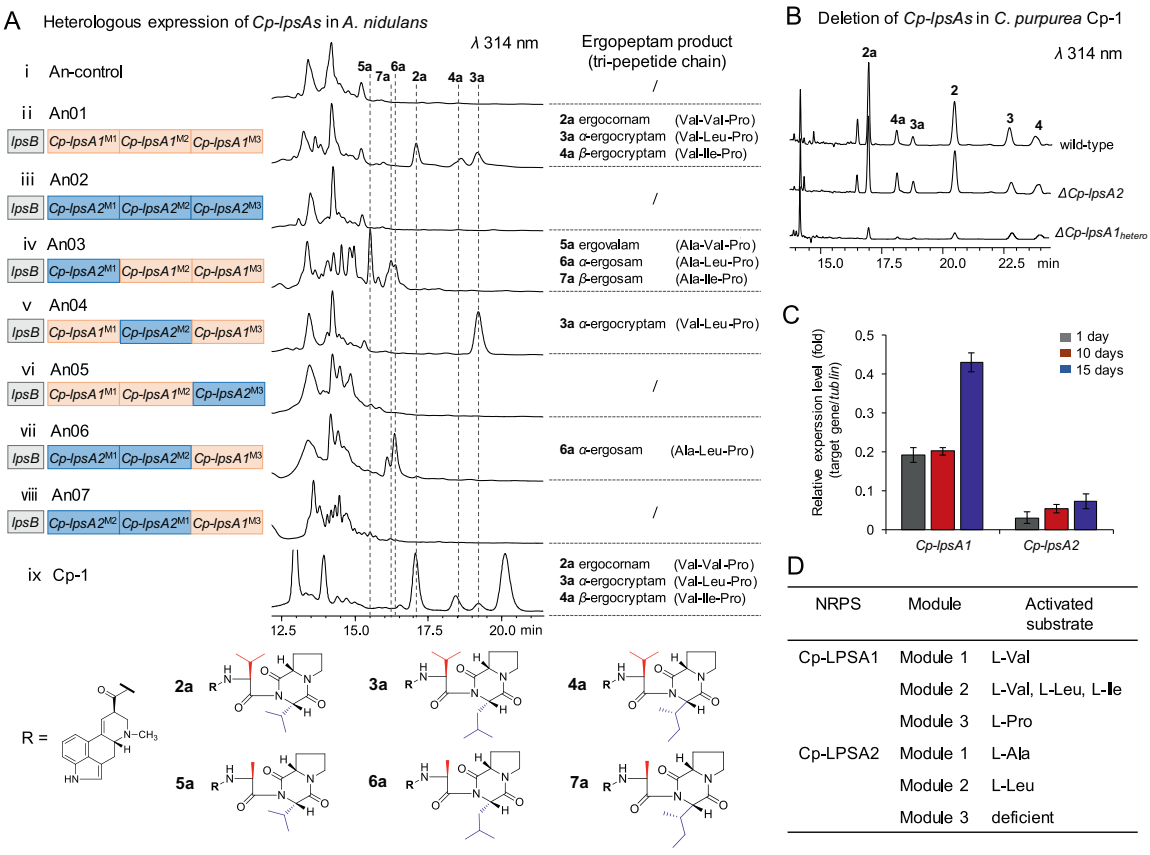

NRPS	Module	Activated substrate
Cp-LPSA1	Module 1	L-Val
	Module 2	L-Val, L-Leu, L-Ile
	Module 3	L-Pro
Cp-LPSA2	Module 1	L-Ala
	Module 2	L-Leu
	Module 3	deficient

Figure 2 Functional characterization of Cp-LPSA1 and Cp-LPSA2 through heterologous expression in *A. nidulans* and gene deletion in *C. purpurea* Cp-1 strain. (A) LC−MS analysis of the product profiles of the recombinant strains An01−An07 that co-expressed *lpsB* with either *Cp-lpsA1* or *Cp-lpsA2,* as well as the recombinant *Cp-lpsAs* with module swapping between *Cp-lpsA1* and *Cp-lpsA2*. (B) HPLC analysis of the product profiles of the wild-type Cp-1 strain and *Cp-lpsA1* and *Cp-lpsA2* knockout mutants. (C) The mRNA expression levels of *Cp-lpsA1* and *Cp-lpsA2* in the wild-type Cp-1 strain at different fermentation stages. The mRNA expression level of the housekeeping gene *tubulin* is set to 1. (D) The activated amino acid substrates for each module of Cp-LPSA1 and Cp-LPSA2 are summarized.

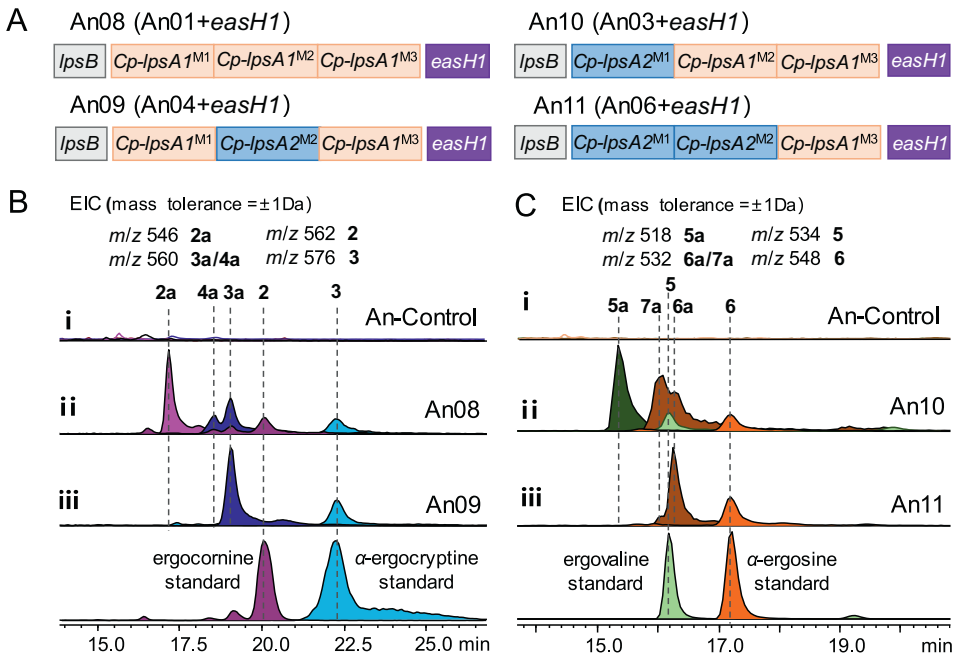

Figure 3 The formation of ergopeptines after introducing oxygenase EasH1 into the corresponding ergopeptam-producing strains. (A) Schematic representation of overexpressed genes in the recombinant strains An08−An11. (B−C) LC−MS analysis of the metabolite profiles of the recombinant strains An08−An11. The extracted ion chromatograms (EICs) were extracted at *m/z* 546 $[M + H]^+$ for **2a**, *m/z* 560 $[M + H]^+$ for **3a** and **4a**, *m/z* 562 $[M + H]^+$ for **2**, *m/z* 576 $[M + H]^+$ for **3**, *m/z* 518 $[M + H]^+$ for **5a**, *m/z* 532 $[M + H]^+$ for **6a** and **7a**, *m/z* 534 $[M + H]^+$ for **5**, *m/z* 548 $[M + H]^+$ for **6.**

some nuclei but still existed in other nuclei within the same cells (Supporting Information Fig. S3). High-performance liquid chromatography (HPLC) analysis of the ethyl acetate extracts from cultures showed that the contents of **2**, **3**, and **4** in the *ΔCp-lpsA1*$_{hetero}$ strain were significantly reduced compared to the wild-type strain, even though the *Cp-lpsA1* gene had not been completely deleted. In contrast, there was no noticeable difference in the *ΔCp-lpsA2* strain (Fig. 2B). In addition, throughout the entire fermentation stages of the wild-type strain, the mRNA expression level of *Cp-lpsA1* was distinctly higher than that of *Cp-lpsA2* (Fig. 2C). These results demonstrated that only Cp-LPSA1 was responsible for the biosynthesis of ergopeptines (**2**, **3** and **4**) in *C. purpurea* Cp-1 strain and the Cp-LPSA2 was inactive. These data were also consistent with the heterologous expression results mentioned above.

Based on the tripeptide chain composition of **2**, **3**, and **4**, it can be concluded that module 1 of Cp-LPSA1 recognizes Val, while module 2 recognizes Val, Leu, or Ile. The first two A domains of Cp-LPSA1 were further expressed and purified, and they contained ten highly conserved regions (motif 1−motif 10) (Supporting Information Fig. S4). *In vitro* activity tests revealed that the first A domain of Cp-LPSA1 (Cp-LPSA1^{Ade1}) exhibited the highest catalytic activity towards Val, while the second A domain of Cp-LPSA1 (Cp-LPSA1^{Ade2}) showed the higher activities towards Leu, Val, and Ile (Supporting Information Fig. S5A), which largely confirmed the function of Cp-LPSA1. It was also noted that Cp-LPSA1^{Ade2} possessed considerable activity towards Ala, but the product with the second amino acid of the tripeptide moiety being Ala was not detected. It implied that the individual structural domain alone could not reflect the enzyme's function.

Collectively, it was confirmed that Cp-LPSA1 catalyzed the formation of **2**, **3**, and **4**. Its first A domain accepted Val, its second A domain accepted any one substrate among Val, Leu, and Ile, while its third A domain accepted Pro (Fig. 2D).

*3.3. Replacing the deficient module 3 of Cp-LPSA2 with a functional one leads to the formation of α-ergosine (**6**)*

To further investigate the function of Cp-LPSA2, the three functional modules of Cp-LPSA2 were respectively utilized to replace their counterparts in Cp-LPSA1. The recombinant Cp-LPSAs were heterologously expressed in *A. nidulans*, generating strains An03−An05. Excitingly, replacing module 1 of Cp-LPSA1 with that of Cp-LPSA2 led to the accumulation of three additional products (**5a**, **6a**, and **7a**) in strain An03 compared to the control strain (Fig. 2Ai and 2Aiv). These products were identified as ergovalam (**5a**), α-ergosam (**6a**), and β-ergosam (**7a**) through LC−MS detection, comparative MS/MS fragmentation analysis, and NMR analysis of the final ergopeptine products (Fig. 3C, Supporting Information Figs. S6-S8, S21-S24, Table S7). Especially, **5a** and **6a** were further converted into ergovaline (**5**) and α-ergosine (**6**), respectively, following the action of EasH1 in An10 (Fig. 3A and Cii). The identification of **6a** was also confirmed by the product analysis of the recombinant strain An11, which produced only **6** (Fig. 3A and Ciii). Consequently, **7a** was inferred to be β-ergosam. Since the first amino acid of the cyclic peptide moieties of **5a**, **6a**, and **7a** was Ala, the first A domain of Cp-LPSA2 was demonstrated to specifically activate Ala. Similarly, replacing module 2 of Cp-LPSA1 with that of Cp-LPSA2 resulted in the production of **3a** in strain An04 (Fig. 2Av), indicating that

the second A domain of Cp-LPSA2 specifically activated Leu. The purified first two A domains of Cp-LPSA2 (Cp-LPSA2^{Ade1} and Cp-LPSA2^{Ade2}) exhibited the highest activities towards Ala and Leu *in vitro*, respectively (Supporting Information Fig. S5B). As the first two modules of Cp-LPSA2 were specific to Ala and Leu, respectively, the normal Cp-LPSA2 should be able to catalyze the formation of **6a** if module 3 could recognize substrate Pro.

Next, we focused on the function of its module 3 of Cp-LPSA2 and replaced the module 3 of Cp-LPSA1 with that of Cp-LPSA2. It was found that the activity of the recombinant enzyme in strain An05 was almost lost (Fig. 2Avi), and only a trace amount of products were detectable through EIC (Supporting Information Fig. S9), indicating that module 3 of Cp-LPSA2 was inefficient, which led to the functional loss of Cp-LPSA2. As expected, the activity of Cp-LPSA2 could be apparently restored by replacing its module 3 with that of Cp-LPSA1, as evidenced by the generation of the expected product **6a** and **6** in the recombinant strains An06 and An11, respectively (Figs. 2Avii and 3Ciii). This observation once again confirmed that the first two modules of Cp-LPSA2 were specific to Ala and Leu, respectively, endowing Cp-LPSA2 with the capacity to synthesize **6** when module 3 was normalized (Fig. 2D). Later, the sequence identity of module 3 between Cp-LPSA1 and Cp-LPSA2 was also compared, and it was found that the sequence identity between the two modules was 94.83%, with the ten specific sites responsible for recognizing Pro remaining unchanged (Supporting Information Fig. S10). The reason for the deficiency of module 3 in Cp-LPSA2 needs to be further investigated.

In addition, we also attempted to swap the positions of modules 1 and module 2 of Cp-LPSA2 to observe if the recombinant enzyme could be functional. Unfortunately, no product was detected in the recombinant strain An07 (Fig. 2Aviii), suggesting that the biosynthesis of ergopeptines was of directionality from module 1 through module 2 to module 3.

*3.4. P1-LPSA1 and P1-LPSA2 are respectively involved in the formation of ergotamine (**9**) and α-ergocryptine (**3**)*

A previous study reported that P1-LPSA1 (GenBank accession no. AJ011964.1) from *C. purpurea* P1 strain was responsible for producing ergotamine (**9**) (the cyclopeptide: Ala-Phe-Pro), as evidenced by gene deletion[35]. Meanwhile, P1-LPSA2 (GenBank accession no. AJ884678.1) was deduced to be involved in the biosynthesis of α-ergocryptine (**3**) (the cyclopeptide: Val-Leu-Pro)[35], but lacking substantive supporting evidence. The aforementioned platform was also used to examine the functions of the P1-LPSA1 and P1-LPSA2. Since the original strain was not available, we had to download the relevant sequences from the NCBI database and synthesize them. The *P1-lpsA1* and *P1-lpsA2*, along with the *lps*B of the Cp-1 strain, were individually expressed in *A. nidulans* to generate recombinant strains. Unfortunately, no product accumulation was observed in any of the recombinant strains (Supporting Information Fig. S11), indicating that the registered data in the NCBI database should be incorrect. Thus, the functions of individual modules of P1-LPSAs were examined by combining these modules with the validated functional modules of Cp-LPSAs to form the chimeric enzymes.

Firstly, we checked the module 1 functions of P1-LPSA1 and P1-LPSA2 by combining each of the modules 1 with modules 2 and 3 of Cp-LPSAs. Sequence analysis revealed that *P1-lpsA1* lacked 767 bp at the 5′ end compared to other LPSA sequences (Supporting Information Fig. S12A), which could lead to its inactivity. We constructed two chimeric enzymes: P1-LPSA1^{M1}Cp-LPSA2^{M2}Cp-LPSA2^{M3} (where P1-LPSA1^{M1} lacks 767 bp) and P1-LPSA1$^{M1}{}_{m}$Cp-LPSA2^{M2}Cp-LPSA2^{M3} (where P1-LPSA1$^{M1}{}_{m}$ includes the restored 767 bp derived from homologous sequence of *Cp-lpsA2*). Our results demonstrated that the latter enzyme could produce **6a** (the cyclopeptide: Ala-Leu-Pro), confirming that this 767 bp sequence was crucial for the activity of module 1 in P1-LPSA1, specifically recognizing Ala (Fig. 4Ai–iii). In addition, the chimeric enzyme P1-LPSA2^{M1}Cp-LPSA2^{M2}Cp-LPSA1^{M3} could produce **3a** (the cyclopeptide: Val-Leu-Pro), indicating that module 1 of P1-LPSA2 specifically recognized Val (Fig. 4Aiv). Ala and Val are also the first amino acids of ergotamine and α-ergocryptine cyclopeptides, respectively.

Additionally, module 2 of P1-LPSA1 or P1-LPSA2 was used to replace their counterpart in *Cp-lpsAs*. The results showed that the chimeric enzymes Cp-LPSA1^{M1}P1-LPSA1^{M2}Cp-LPSA1^{M3} in strain An18 and Cp-LPSA2^{M1}P1-LPSA1^{M2}Cp-LPSA1^{M3} in strain An19 led to the formation of ergocristam (**8a**) with the $[M + H]^+$ ion at *m/z* 594 and ergotamam (**9a**) with the $[M + H]^+$ ion at *m/z* 566, respectively (Fig. 4Av–vi, Supporting Information Fig. S13). These compounds were further converted into ergocristine (**8**) and ergotamine (**9**) by introducing oxygenase EasH1 into the corresponding recombinants (Fig. 4B and C). The structures of **8** and **9** were also confirmed by LC–MS detection and NMR analysis (Supporting Information Figs. S13, S25-S30, Tables S8 and S9). These results confirmed that module 2 of P1-LPSA1 specifically recognized Phe. Similarly, the strains An20 and An21, which harbored chimeric enzymes Cp-LPSA1^{M1}P1-LPSA2^{M2}Cp-LPSA1^{M3} and Cp-LPSA2^{M1}P1-LPSA2^{M2}-Cp-LPSA1^{M3}, respectively, produced **3a** and **6a**, indicating that module 2 of P1-LPSA2 specifically recognized Leu (Fig. 4Avii–viii). Phe and Leu are also the second amino acids of ergotamine and α-ergocryptine cyclopeptides, respectively.

We further investigated the functions of module 3 of P1-LPSAs. Sequence alignment analysis revealed that *P1-lpsA1* lacked 363 bp at its 3′ end compared to other *lpsA* sequences (Supporting Information Fig. S12B), which may result in the inactivity of module 3 (Fig. 4Di). Using the homologous sequence from the 3′ end of *Cp-lpsA1* to fill the gap, we constructed the chimeric enzyme Cp-LPSA1^{M1}Cp-LPSA2^{M2}P1-LPSA1$^{M3\#}$ to successfully produce **3a**, indicating that the corrected module 3 of P1-LPSA1 could recognize Pro (Fig. 4Dii). Additionally, sequence analysis showed that module 3 of *P1-lpsA2* contained an additional 16 bases of discontinuous insertions and one base of deletion compared to the other reported *lpsAs*, which might potentially cause the downstream mutation (Supporting Information Fig. S14). Furthermore, *P1-lpsA2* also lacked a length of 118 bp at its 3′ end compared to other *lpsA* sequences (Fig. S12B). To address these abnormal changes, we first synthesized a modified version of *P1-lpsA2^{M3}**, in which the additional 16 bases of discontinuous insertions and one base of deletion were corrected. Based on *P1-lpsA2^{M3}**, we further synthesized a modified version of *P1-lpsA2$^{M3\#}$*, in which the missing 118 bp at the 3′ end was compensated by using the homologous sequence. The two modified third modules were used to construct the following chimeric enzymes: P1-LPSA2^{M1}P1-LPSA2^{M2}P1-LPSA2^{M3}*, Cp-LPSA2^{M1}Cp-LPSA2^{M2}P1-LPSA2^{M3}*, Cp-LPSA1^{M1}Cp-LPSA2^{M2}P1-LPSA2^{M3}*, and Cp-LPSA1^{M1}Cp-LPSA2^{M2}P1-LPSA2$^{M3\#}$. Unfortunately, none of these chimeric enzymes could synthesize the corresponding ergopeptams (Fig. 4Diii–v, Supporting Information Fig. S11), indicating that the other errors

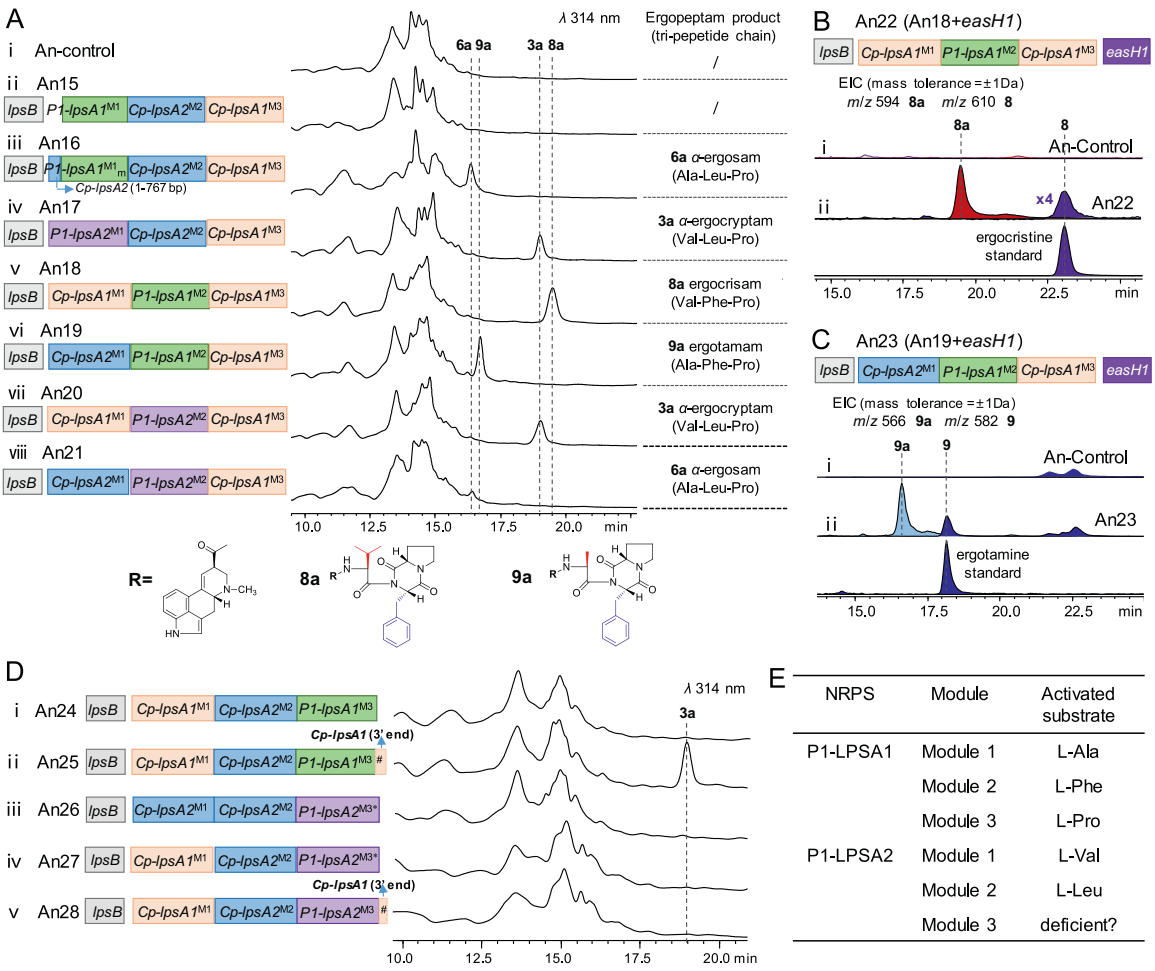

Figure 4 Functional characterization of P1-LPSA1 and P1-LPSA2 through heterologous expression in *A. nidulans*. (A) LC−MS analysis of the product profiles of the recombinant strains An15−An21, which coexpressed *lpsB* and chimeric *lpsAs* constructed by combining module 1 or module 2 from P1-LPSAs with functional modules from Cp-LPSAs. (B, C) LC−MS analysis of the product profiles of the recombinant strains An22 and An23, which introduced oxygenase EasH1 into An18 and An19, respectively. The extracted ion chromatograms (EICs) were extracted at *m/z* 594 $[M + H]^+$ for **8a**, *m/z* 610 $[M + H]^+$ for **8**, *m/z* 566 $[M + H]^+$ for **9a**, *m/z* 582 $[M + H]^+$ for **9.** (D) LC−MS analysis of the product profiles of the recombinant strains An24−An28, which coexpressed *lpsB* and chimeric *lpsAs* constructed by combining module 3 of P1-LPSAs with functional modules from Cp-LPSAs. *P1-lpsA2*^{M3*} refers to corrections made for excess base insertions or deletion at various positions in module 3 of *P1-lpsA2*; *P1-lpsA1*$^{M3\#}$ and *P1-lpsA2*$^{M3\#}$ indicate that the homologous sequences from the 3′ end of *Cp-lpsA1* were used to fill gaps present in *P1-lpsA1*^{M3} and *P1-lpsA2*^{M3*}, respectively. (E) The activated amino acid substrates for each module of P1-LPSA1 and P1-LPSA2 are summarized.

still existed in the NCBI registered sequence. Briefly, except the registered module 3 of P1-LPSA2, all other modules of P1-LPSAs have been characterized in terms of their substrate specificities, in which modules 1, 2 and 3 of P1-LPSA1 recognized Ala, Phe and Pro [three amino acids of ergotamine (**9**) cyclopeptide], respectively, while the modules 1 and 2 of P1-LPSA2 recognized Val and Leu [first two amino acids of α-ergocryptine (**3**) cyclopeptide], respectively (Fig. 4E).

3.5. Exploration of key sites involved in substrate specificity of LPSAs

Ten key positions relevant to substrate specificity have been identified within A domains in NRPS[46], and the amino acid residues occupying these positions were collectively referred to as the non-ribosomal peptide code (NRP code)[47,48]. These NRP codes within the LPSAs from Cp-1 and P1 strains were compared (Fig. 5A). The sequence identity of these key sites in the first two A domains was lower, whereas the corresponding sites in the third A domain were identical because the binding substrate was Pro.

In module 1, the NRP codes in Cp-LPSA1 and P1-LPSA2 were identical ($D^{192}A^{193}I^{196}F^{233}C^{254}G^{256}G^{277}P^{285}L^{286}K^{517}$), specifically recognizing Val. Similarly, the NRP codes in module 1 of Cp-LPSA2 and P1-LPSA1 were also the same ($D^{192}L^{193}F^{196}F^{233}C^{254}G^{256}G^{277}P^{285}L^{286}K^{517}$), and both modules activated Ala (Fig. 5A). The sequence identity of NRP codes in module 2 of LPSAs was lower, and this module was crucial in determining the diversity of ergopeptine profiles between different *C. purpurea* strains. Comparison of the NRP codes in module 2 of Cp-LPSA1 and P1-LPSA1 revealed differences in five residues

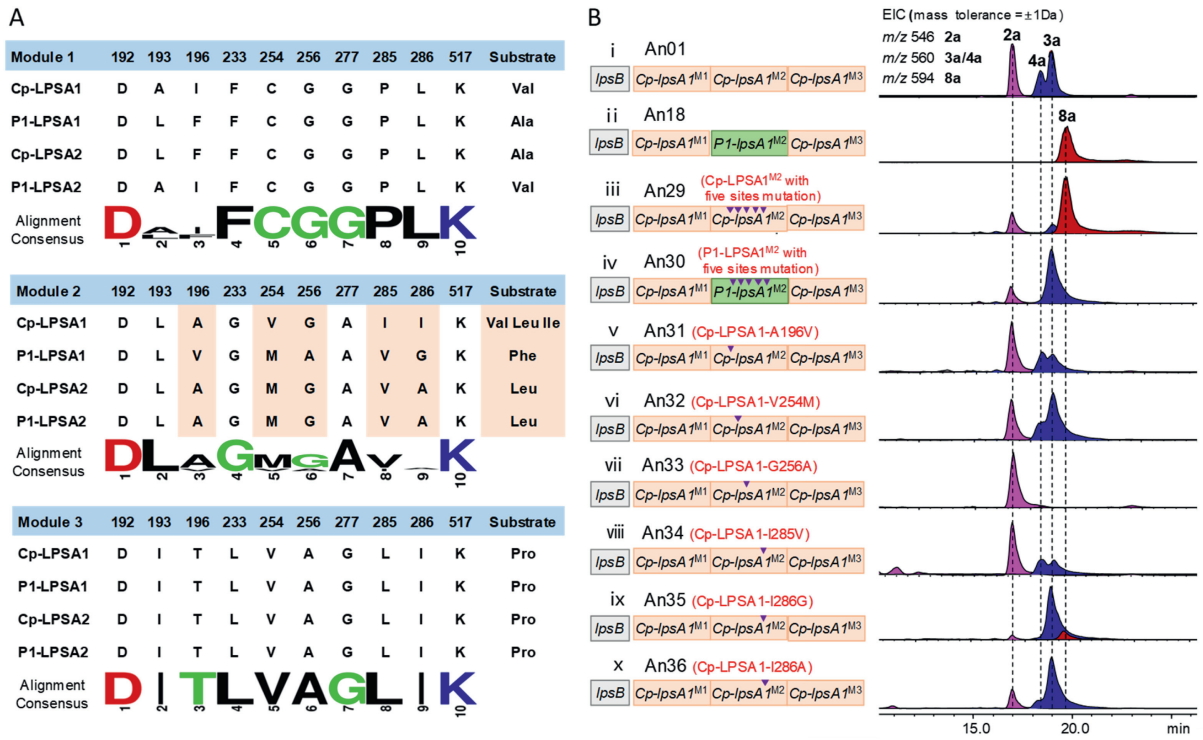

Figure 5 Exploration of the key sites involved in substrate specificity of LPSAs. (A) Sequence alignment of the specificity-determining residues in A domains of LPSAs from *C. purpurea* Cp-1 and P1 strain. The amino acid sequences of A domains were submitted to the web-based NRPS predictor2 tool, and the 10 amino acid codes of the A domains were extracted. (B) LC−MS analysis of the metabolite profiles of the recombinant strains An29−An36 that coexpressed *lpsB* and *lpsA* mutants. The extracted ion chromatograms (EICs) were extracted at *m/z* 546 $[M + H]^+$ for **2a**, *m/z* 560 $[M + H]^+$ for **3a** and **4a**, *m/z* 594 $[M + H]^+$ for **8a**. Purple triangle indicates the mutation site.

(Fig. 5A), which might be the key sites leading to the recognition of different substrates. It was hypothesized that if these five differential residues in Cp-LPSA1 (A196, V254, G256, I285 and I286) were mutated into corresponding residues at the equivalent positions in P1-LPSA1 (V196, M254, A256, V285 and G286), the ergopeptine profiles might be switched from the product synthesized by Cp-LPSA1 to that of P1-LPSA1. Encouragingly, our result confirmed this prediction. In the recombinant strain An29 harboring the pentameter mutant Cp-LPSA1^{M1}Cp-LPSA1$^{M2-penta}$Cp-LPSA1^{M3} (where Cp-LPSA1$^{M2-penta}$ indicated that Cp-LPSA1^{M2} contained five point mutations: A196V, V254M, G256A, I285V, and I286G), the production of **2a**, **3a**, and **4a** was significantly reduced, while **8a** was produced at a content of 71.45% (Fig. 5Bi−iii, Supporting Information Table S5). Likewise, the five differential residues in P1-LPSA1 were mutated into the corresponding residues in Cp-LPSA1, generating the pentameter mutant Cp-LPSA1^{M1}P1-LPSA1$^{M2-penta}$Cp-LPSA1^{M3} (where P1-LPSA1$^{M2-penta}$ indicated that P1-LPSA1^{M2} contained five point mutations: V196A, M254V, A256G, V285I, and G286I). The recombinant strain An30 harboring this chimeric enzyme almost lost the ability to synthesize **8a** but produced **2a** and **3a** (Fig. 5Biv, and Table S5). These results confirmed that the combinatorial directed mutagenesis of these differential sites among NRP codes could change substrate specificity. The homology models of the second A domain of Cp-LPSA1 (Cp-LPSA1^{Ade2}) and P1-LPSA1(P1-LPSA1^{Ade2}) were constructed to reveal the molecular mechanism underlying their substrate specificity. The binding pockets of Cp-LPSA1^{Ade2} and P1-LPSA1^{Ade2} were surrounded mainly by the ten key sites, most of which were hydrophobic residues except D192 and K517. The binding pocket of P1-LPSA1^{Ade2} was more spacious than that of Cp-LPSA1^{Ade2} due to residues at positions 285 and 286 with relatively short side chains, which might provide additional flexibility to accommodate Phe with a bulky phenyl ring structure (Fig. 6A).

Unlike other reported modules with rigid substrate specificity, module 2 of Cp-LPSA1 accepted three structurally similar amino acids, exhibiting relatively broad substrate specificity. Further site-directed mutagenesis experiments were conducted to identify the residue determining ergopeptine formation in Cp-LPSA1. The five differential sites in module 2 of Cp-LPSA1 (template) were mutated towards their counterparts P1-LPSA1 or Cp-LPSA2, generating strains An31−An36. Among the mutants with single point mutations from Cp-LPSA1 to P1-LPSA1, only the I286G mutation in Cp-LPSA1 could produce a small amount of **8a** (Fig. 5Bix). This might be due to the mutation of the residue at position 286 to Gly, which had the smallest side chain, allowing for the expansion of the active cavity (Supporting Information Fig. S15D), and providing conditions for accommodating Phe. Among the mutants with single-point mutations from Cp-LPSA1 to Cp-LPSA2, the V254M or I286A mutation in Cp-LPSA1 showed a significant increase in the levels of **3a** (Fig. 5Bvi and 5Bx), particularly the latter. Specifically, the I286A mutation increased the content of **3a** from 33.6% to 81.1% (Table S5), indicating enhanced affinity of this mutant for Leu. Regarding the change in substrate affinity, the following speculations were put forward. When Ile286 in Cp-LPSA1 was mutated into an amino acid with a smaller side chain, such as Ala, the binding pocket became larger, potentially allowing for easier entry of Leu (Supporting Information Fig. S15C). Moreover, the docking model of the enzyme-aminoacyl-AMP complex indicated that the mutant

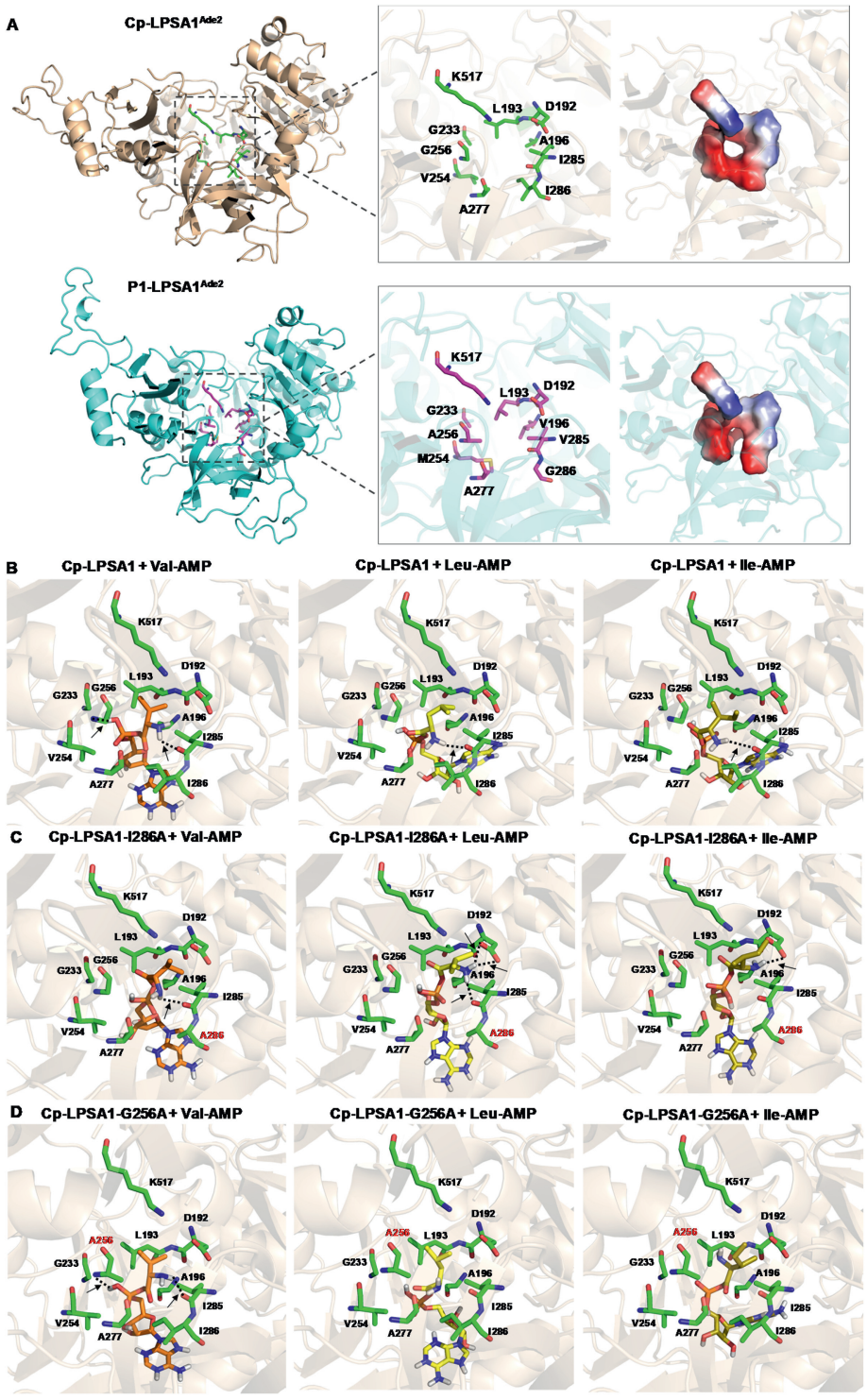

Figure 6 Structural prediction of the second A domain of LPSA and protein-substrate docking analysis. (A) The homology model of the second A domain of Cp-LPSA1 (Cp-LPSA1^{Ade2}) and P1-LPSA1 (P1-LPSA1^{Ade2}). The 3D dimensional structures of Cp-LPSA1^{Ade2} and P1-LPSA1^{Ade2} were predicted using the Swiss Model, based on the template, A domain of gramicidin synthetase 1 (PDB ID: 1AMU). The overall structures of all proteins are shown as cartoon. The ten key positions determining substrate specificity are shown in stick form and labeled accordingly. The binding pockets of A domain surrounded by these ten key sites were generated in PyMOL. (B—D) Partial view of enzyme-aminoacyl-AMP docking. Hydrogen bonds were formed between the amino acid residues that compose the binding pocket of Cp-LPSA1, Cp-LPSA1-I286A, and Cp-LPSA1-G256A with aminoacyl-AMP. The ten key positions determining substrate specificity are shown in green and labeled accordingly. Hydrogen bonds are shown as dotted lines. The substrate Val-AMP, Leu-AMP, and Ile-AMP are shown in orange, yellow, and oliver, respectively.

with I286A mutation might have a stronger interaction with Leu (three hydrogen bonds formed among Leu-AMP with D192 and I285) than with Val or Ile (Fig. 6B and C).

Furthermore, it was found that the G256A mutation in Cp-LPSA1 predominantly produced **2a**, indicating that the mutated module 2 almost exclusively recognized Val, rather than the initial three substrates (Fig. 5Bvii and Table S5). The possible reason for the phenomenon was that the G256A mutation made the binding pocket smaller (Supporting Information Fig. S15B), which was not conducive to the entry of Leu/Ile with longer side chains but facilitated the entry of Val. In addition, the G256A mutant had a stronger interaction with Val (two hydrogen bonds formed among Val-AMP with A256 and I285) than with Leu or Ile (Fig. 6D). Further investigations, such as solving the crystal structure, would help elucidate the molecular mechanism.

*3.6. Mixed-culture of C. paspali and recombinant A. nidulans for the production of α-ergocryptine (**3**) and ergotamine (**9**)*

Within the *Claviceps* genus, *Claviceps paspali* can not produce ergopeptines due to the absence of *lpsAs*. The *C. paspali* No. 24 strain, a mutant isolated and preserved in our lab, exclusively produced D-lysergic acid at 24.4 mg/L (Supporting Information Fig. S16). To omit the D-lysergic acid feeding and efficiently obtain **3**, a mixed-culture platform of *C. paspali*−*A. nidulans* was designed (Fig. 7A), and the *C. paspali* No. 24 strain was utilized to supply the substrate D-lysergic acid, while the An09 (the recombinant *A. nidulans* strain overexpressing the chimeric enzyme Cp-LPSA1^{M1}Cp-LPSA2^{M2}Cp-LPSA1^{M3}, LPSB and EasH1) was dedicated to convert D-lysergic acid to **3**, a precursor for clinical drugs such as α-dihydroergocryptine and bromocriptine. Initially, *C. paspali* No. 24 and the An09 strains were fermented separately for 10 days and 2 days, respectively. Subsequently, they were co-cultivated for 2 days at different ratios of inoculation volumes ($V_{C.\ paspali}$:$V_{A.\ nidulans}$). As shown in Fig. 7B, the production of **3a** and **3** varied with the inoculation ratios. Co-cultivation at an incubation ratio of 1:1 (C2 group) produced **3a** and **3** at 0.47 ± 0.09 and 0.84 ± 0.11 mg/L, respectively, which was 1.9 and 1.5 times higher than compared to the initial inoculation ratio of 1:2 (C1 group). Furthermore, the fermentation supernatant of *C. paspali* No. 24, either at half volume (C3 group) or equal volume (C4 group), was added to the 2-day culture of the An09 strain. It was found that this method significantly enhanced the production of **3a** and **3**. In the C4 group, the yields of **3a** and **3** reached 0.65 ± 0.11 and 1.46 ± 0.11 mg/L, respectively, representing 2.7 and 2.6 times higher than the C1 group. Similarly, adding an equal volume of *C. paspali* No. 24 fermentation supernatant to recombinant *A. nidulans* An23 (which overexpressed the chimeric enzyme Cp-LPSA2^{M1}P1-LPSA1^{M2}Cp-LPSA1^{M3}, LPSB, and EasH1 and was responsible for producing the clinical drug **9**), yielded 0.49 ± 0.13 mg/L **9a** and 1.09 ± 0.14 mg/L **9**, respectively (Fig. 7C).

4. Discussion

The ergopeptine profiles among different *C. purpurea* strains exhibited considerable diversity, and more than two types of ergopeptines were usually produced within the same strain, all of which were associated with the two LPSA members in each strain. During the bicyclic tripeptide formation, the first two amino acids were respectively determined by the first two modules of the LPSA members while the third module always recognized Pro. However, there has been a lack of systematic characterization regarding how LPSA members precisely control the types of synthesized ergopeptines. In this study, the two new LPSA members *Cp-lpsA1* and *Cp-lpsA2* were firstly cloned from *C. purpurea* Cp-1 strain, and they only kept 84.6%−94.8% amino acid sequence identity with other reported LPSAs. The sequence heterogeneity of *Cp-lpsA1* and *Cp-lpsA2* might contribute to the varying product spectra observed between the Cp-1 strain and other reported *C. purpurea* strains. In addition, the endophytic fungi of the family Clavicipitaceae including *Epichloe* and *Neotyphodium* also produced ergopeptine, mainly ergovaline (**5**)[49]. Phylogenetic analysis showed that the *lpsAs* from *Claviceps* strains were always grouped into one clade in the resultant phylogenetic tree while the *lpsAs* from *Epichloe* and *Neotyphodium* strains formed another clade, implying that the variations in *lpsAs* among different species of Clavicipitaceae determined the types of synthesized ergopeptines (Supporting Information Fig. S17).

The *A. nidulans* heterologous expression system was chosen to further investigate the functions of Cp-LPSAs for the following

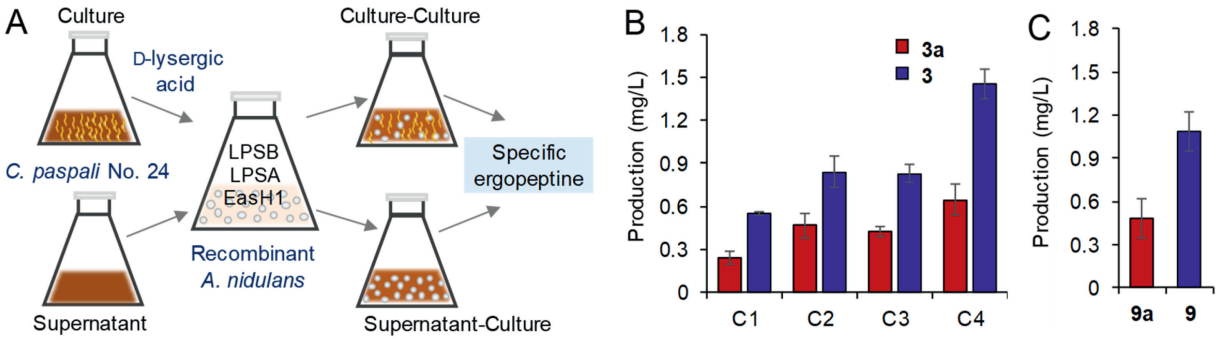

Figure 7 Mixed-culture of *C. paspali* and *recombinant A. nidulans* for the production of specific ergopeptines. (A) Schematic representation of the *C. paspali*-recombinant *A. nidulans* co-culture system for ergopeptine biosynthesis. (B) Production of **3a** and **3** using different mixed-culture methods. C1 group, co-cultivation of *C. paspali* No. 24 and recombinant *A. nidulans* An09 at 2:1 ratio of incubation volumes; C2 group, co-cultivation of *C. paspali* No. 24 and recombinant *A. nidulans* An09 at 1:1 ratio of incubation volumes; C3 group, addition of half volume of *C. paspali* No. 24 fermentation supernatant to recombinant *A. nidulans* An09; C4 group, addition of equal volume of *C. paspali* No. 24 fermentation supernatant to recombinant *A. nidulans* An09. (C) Production of **9a** and **9** by adding an equal volume of *C. paspali* No. 24 fermentation supernatant to recombinant *A. nidulans* An23.

reasons: (1) *A. nidulans* itself did not produce ergot alkaloids, ensuring a clean genetic background that did not interfere with the study of the biosynthesis of ergopeptines; (2) *A. nidulans* possessed a native gene-splicing system[38], facilitating the recognition of introns from other fungal genes, including those from *Claviceps* species, ensuring correct gene splicing of giant LPSA genes; (3) By providing lysergic acid and utilizing its cellular amino acid pool, the synthesis of ergopeptams, the direct precursors of the corresponding ergopeptines, could be achieved in *A. nidulans*. Through heterologous expression in *A. nidulans,* we proved that Cp-LPSA1 from *C. purpurea* Cp-1 strain was responsible for the biosynthesis of three ergopeptines (**2**–**4**), while the ability of Cp-LPSA2 to synthesize **6** was restored by replacing its deficient module 3 with that of Cp-LPSA1. It had previously been proposed that LPSA1 and LPSA2 arose from a gene duplication event, with only one of them being highly expressed, resulting in one type of ergopeptine being the main component in the total products[20]. Our findings highlighted the crucial role of Cp-LPSA1 in ergopeptine biosynthesis in the Cp-1 strain, as it was evident from its significant mRNA expression level and enzyme

A

Chimeric enzyme						Product
Module 1		Module 2		Module 3		
Cp-lpsA1^{M1} (A$_1$T$_1$C$_1$)	L-Val	*Cp-lpsA1*^{M2} (A$_2$T$_2$C$_2$)	L-Val L-Leu L-Ile	*Cp-lpsA1*^{M3} (A$_3$T$_3$C$_3$)	L-Pro	**2a** ergocornam **3a** *α*-ergocryptam **4a** *β*-ergocryptam
Cp-lpsA1^{M1} (A$_1$T$_1$C$_1$)	L-Val	*Cp-lpsA1*$^{M2\text{-}G256A}$ (A$_2$T$_2$C$_2$)	L-Val	*Cp-lpsA1*^{M3} (A$_3$T$_3$C$_3$)	L-Pro	**2a** ergocornam
Cp-lpsA1^{M1} (A$_1$T$_1$C$_1$)	L-Val	*Cp-lpsA2*^{M2} (A$_2$T$_2$C$_2$)	L-Leu	*Cp-lpsA1*^{M3} (A$_3$T$_3$C$_3$)	L-Pro	**3a** *α*-ergocryptam
P1-lpsA2^{M1} (A$_1$T$_1$C$_1$)	L-Val	*Cp-lpsA2*^{M2} (A$_2$T$_2$C$_2$)	L-Leu	*Cp-lpsA1*^{M3} (A$_3$T$_3$C$_3$)	L-Pro	
Cp-lpsA1^{M1} (A$_1$T$_1$C$_1$)	L-Val	*P1-lpsA2*^{M2} (A$_2$T$_2$C$_2$)	L-Leu	*Cp-lpsA1*^{M3} (A$_3$T$_3$C$_3$)	L-Pro	
Cp-lpsA1^{M1} (A$_1$T$_1$C$_1$)	L-Val	*P1-lpsA1*^{M2} (A$_2$T$_2$C$_2$)	L-Phe	*Cp-lpsA1*^{M3} (A$_3$T$_3$C$_3$)	L-Pro	**8a** ergocristam
Cp-lpsA2^{M1} (A$_1$T$_1$C$_1$)	L-Ala	*Cp-lpsA1*^{M2} (A$_2$T$_2$C$_2$)	L-Val L-Leu L-Ile	*Cp-lpsA1*^{M3} (A$_3$T$_3$C$_3$)	L-Pro	**5a** ergovalam **6a** *α*-ergosam **7a** *β*-ergosam
Cp-lpsA2^{M1} (A$_1$T$_1$C$_1$)	L-Ala	*Cp-lpsA1*$^{M2\text{-}G256A}$ (A$_2$T$_2$C$_2$)	L-Val	*Cp-lpsA1*^{M3} (A$_3$T$_3$C$_3$)	L-Pro	**5a** ergovalam
Cp-lpsA2^{M1} (A$_1$T$_1$C$_1$)	L-Ala	*Cp-lpsA2*^{M2} (A$_2$T$_2$C$_2$)	L-Leu	*Cp-lpsA1*^{M3} (A$_3$T$_3$C$_3$)	L-Pro	
Cp-lpsA2^{M1} (A$_1$T$_1$C$_1$)	L-Ala	*P1-lpsA2*^{M2} (A$_2$T$_2$C$_2$)	L-Leu	*Cp-lpsA1*^{M3} (A$_3$T$_3$C$_3$)	L-Pro	**6a** *α*-ergosam
P1-lpsA1$^{M1}{}_m$ (A$_1$T$_1$C$_2$)	L-Ala	*Cp-lpsA2*^{M2} (A$_2$T$_2$C$_2$)	L-Leu	*Cp-lpsA1*^{M3} (A$_3$T$_3$C$_3$)	L-Pro	
Cp-lpsA2^{M1} (A$_1$T$_1$C$_1$)	L-Ala	*P1-lpsA1*^{M2} (A$_2$T$_2$C$_2$)	L-Phe	*Cp-lpsA1*^{M3} (A$_3$T$_3$C$_3$)	L-Pro	**9a** ergotamam

B

Module 1	Module 2				Module 3
	D^{192}L^{193}A^{196}G^{233} V^{254}G^{256}A^{277}I^{285} I^{286}K^{517} (**Val/Leu/Ile**)	D^{192}L^{193}A^{196}G^{233} V^{254}A^{256}A^{277}I^{285} I^{286}K^{517} (**Val**)	D^{192}L^{193}A^{196}G^{233} M^{254}G^{256}A^{277}V^{285} A^{286}K^{517} (**Leu**)	D^{192}L^{193}V^{196}G^{233} M^{254}A^{256}A^{277}V^{285} G^{286}K^{517}(**Phe**)	
D^{192}A^{193}I^{196}F^{233} C^{254}G^{256}G^{277}P^{285} L^{286}K^{517} (**Val**)	ergocornine /*α*-ergocryptine /*β*-ergocryptine	ergocornine	*α*-ergocryptine	ergocristine	D^{192}I^{193}T^{196}L^{233} V^{254}A^{256}G^{277}L^{285} I^{286}K^{517} (**Pro**)
D^{192}L^{193}F^{196}F^{233} C^{254}G^{256}G^{277}P^{285} L^{286}K^{517} (**Ala**)	ergovaline /*α*-ergosine /*β*-ergosine	ergovaline	*α*-ergosine	ergotamine	

Figure 8 Production of specific kinds of ergopeptines by module recombination of LPSAs. (A) The biosynthesis of eight specific ergopeptams and six ergopeptines using the chimeric enzymes constructed by combining functional modules of LPSAs with different substrate specificity. *P1-lpsA1*$^{M1}{}_m$ includes the restored missing 767 bp at the 5′ end using the homologous sequence of *Cp-lpsA2*. (B) The summarized "non-ribosomal peptide code table" (NRP code table) for the production of different ergopeptines.

activity (Fig. 2). Moreover, the low mRNA expression level of Cp-LPSA2 suggested that even if it could perform its function correctly, the synthesized product **6** might only account for a small fraction of the total products.

Our research proved that the functional modules of different LPSA members exhibited distinct substrate specificities (Fig. 8A). For module 1, it was mainly responsible for recognizing Ala or Val, as exemplified by Cp-LPSA2 and P1-LPSA1 whose module 1 recognized Ala, while those of Cp-LPSA1 and P1-LPSA2 recognized Val (Figs. 2 and 4). This also clarified why the first amino acid of the circular tripeptide of the reported ergopeptines was mostly Ala or Val. Module 2 of Cp-LPSA2 and P1-LPSA2 specially recognized Leu, while module 2 of P1-LPSA1 specially recognized Phe. However, module 2 of Cp-LPSA1 could recognize three structurally similar amino acids, including Val, Leu, and Ile, ultimately leading to the biosynthesis of three ergopeptines (Figs. 2 and 4). Consequently, these findings elucidated why one strain could produce more than two ergopeptines, and confirmed that different LPSA members had unique substrate specificities, ultimately leading to diverse product profiles among *C. purpurea* strains.

We further analyzed the NRP codes within the different LPSA members. These codes all contained conserved Asp192 and Lys517. Asp192 served as a general signature for recognizing amino acid substrates and stabilized the α-amino group of substrates, while Lys517 was a highly conserved site that mediated key interactions with both the amino and carboxyl groups of substrates[29,50]. In module 1 of different LPSA members, there were two types of NRP codes, referred to as $D^{192}A^{193}I^{196}F^{233}C^{254}G^{256}G^{277}P^{285}L^{286}K^{517}$ and $D^{192}L^{193}F^{196}F^{233}C^{254}G^{256}G^{277}P^{285}L^{286}K^{517}$, which were involved in the recognition of Val and Ala, respectively. The second amino acid in the tripeptide moiety of naturally occurring ergopeptines reported was frequently Val, Leu, Ile, and Phe, indicating that module 2 of LPSA members recognized a broader range of amino acid substrates. By studying the function of LPSA members in the Cp-1 and P1 strains, it was confirmed that the NRP code $D^{192}L^{193}A^{196}G^{233}V^{254}G^{256}A^{277}I^{285}I^{286}K^{517}$ within module 2 participated in recognizing structurally similar Val, Ile, and Leu. Additionally, the code $D^{192}L^{193}A^{196}G^{233}M^{254}G^{256}A^{277}V^{285}A^{286}K^{517}$ was involved in specific recognition of Leu, while the code $D^{192}L^{193}V^{196}G^{233}M^{254}A^{256}A^{277}V^{285}G^{286}K^{517}$ was involved in specific recognition of Phe. Our study demonstrated that combinatorial mutations of differential sites among NRP codes within module 2 of Cp-LPSA1 and P1-LPSA1 could shift their substrate specificity. Furthermore, it was found that the single-point mutations at positions 256 and 286 in module 2 of Cp-LPSA1 could alter substrate specificity (Fig. 5). Specifically, the G256A mutation enabled the enzyme to predominantly recognize Val, resulting in the exclusive production of **2a**. Based on this, it was concluded that this "unnatural" NRP code $D^{192}L^{193}A^{196}G^{233}V^{254}A^{256}A^{277}I^{285}I^{286}K^{517}$ was involved in specific recognition of Val. The recombinant enzyme Cp-LPSA2^{M1}Cp-LPSA1$^{M2\text{-}G256A}$Cp-LPSA1^{M3} catalyzed the formation of **5a** (Supporting Information Fig. S18), which also confirmed this observation. The above findings also suggested that certain key residues within the NRP codes played a key role in substrate specificity and product interconversion.

Currently, the main method for producing bioactive ergopeptines is through liquid fermentation of *C. purpurea*. However, *C. purpurea* frequently produces multiple ergopeptines with similar structures simultaneously, which complicates the subsequent separation and preparation of the desired ergopeptine. Therefore, achieving directed biosynthesis of ergot alkaloids is of great significance. In this study, by recombining or rationally designing different modules of LPSAs, we demonstrated that the constructed chimeric enzymes could produce specific ergopeptams and the corresponding ergopeptines, including ergocornine (**2**), α-ergocryptine (**3**), ergovaline (**5**), α-ergosine (**6**), ergocristine (**8**), and ergotamine (**9**) (Fig. 8A), which can be used for the semi-synthesis of clinical drugs such as α-dihydroergocryptine, bromocriptine, and dihydroergotamine, or follow-up drug development. Based on these findings, we have also summarized a "non-ribosomal peptide code table" (NRP code table) for the production of different ergopeptines (Fig. 8B). Especially, the production of **3** and **9** reached 1.46 and 1.09 mg/L, respectively, by mixed-culture of *C. paspali* and *A. nidulans* recombinants (Fig. 7). Currently, a research group has established the biosynthetic pathway of D-lysergic acid in *A. nidulans*, but an only trace amount of D-lysergic acid was detected[38]. Subsequently, another research group reported *de novo* heterologous biosynthesis of D-lysergic acid in *S. cerevisiae*, with a yield of 1.7 mg/L[26]. If LPSB, LPSA, and EASH1 were further introduced into these systems, it would probably be challenging to produce ergopeptine. Therefore, compared to these reports, our platform has certain advantages for the directed production of targeted ergopeptines, although the yields we have achieved so far are still relatively low. In the future, effective strategies need to be explored to further increase the yields, such as increasing the supply of D-lysergic acid, enhancing the activity of rate-limiting enzymes like EasH1, or optimizing co-cultivation conditions. Additionally, we may consider developing the chassis of *C. paspali* and construct the biosynthetic pathway in the host for *de novo* production of desired ergopeptines.

5. Conclusions

In conclusion, we systematically characterized the referred LPSA members involved in synthesizing different ergopeptines and clarified that only the LPSA could determine the ergopeptine spectra of the *C. purpurea* strains. Specifically, our findings demonstrated that the three A domains of LPSA members exhibited a certain substrate specificity, precisely controlling the types of ergopeptines synthesized and diverse product spectra among different *C. purpurea* strains or even within the same strain. Additionally, we identified key amino acid residues (or sites) involved in the substrate specificity of LPSA members, which could be targeted for rational design to manipulate substrate selectivity. More importantly, LPSA functional modules with different substrate specificities could be recombined to construct the chimeric LPSAs for producing the specific ergopeptines. To the best of our knowledge, this is the first systematic study on the biosynthetic mechanisms of ergopeptines using heterologeous expression systems. This platform enables the characterization of any LPSAs from ergot fungus and allows for detecting and correcting naturally deficient modules. Our study not only deepens the understanding of the biosynthesis of ergopeptines but also facilitates the re-engineering of LPSAs to achieve the directed biosynthesis of desired ergopeptines or discover more clinically effective analogs in the future.

Acknowledgments

This study was supported by the Beijing Natural Science Foundation (Grant no. 7252205), the CAMS Innovation Fund for Medical Sciences (Grant no. CIFMS2021-I2M-1-029), and the National Natural Science Foundation of China (Grant no. 81603002). We are grateful to Prof. Yi Tang from the University

of California, Los Angeles for providing *Aspergillus nidulans* heterologous expression host and the related plasmids.

Author contributions

Jing−Jing Chen and Ping Zhu designed the research. Jing−Jing Chen carried out the experiments and performed data analysis. Wei-Bo Wang and Ting Gong participated part of the experiments. Jing−Jing Chen wrote the manuscript. Ting Gong, Tian-Jiao Chen, Jin-Ling Yang, and Ping Zhu revised the manuscript. All of the authors have read and approved the final manuscript.

Conflicts of interest

The authors declare no conflicts of interest to declare.

Appendix A. Supporting information

Supporting information to this article can be found online at https://doi.org/10.1016/j.apsb.2025.03.022.

References

1. Panaccione DG. Derivation of the multiply-branched ergot alkaloid pathway of fungi. *Microb Biotechnol* 2023;**16**:742−56.
2. Uhlig S, Rangel-Huerta OD, Divon HH, Rolén E, Pauchon K, Sumarah MW, et al. Unraveling the ergot alkaloid and indole diterpenoid metabolome in the *Claviceps purpurea* species complex using LC−HRMS/MS diagnostic fragmentation filtering. *J Agric Food Chem* 2021;**69**:7137−48.
3. Agriopoulou S. Ergot alkaloids mycotoxins in cereals and cereal-derived food products: characteristics, toxicity, prevalence, and control strategies. *Agronomy* 2021;**11**:931.
4. Jamieson CS, Misa J, Tang Y, Billingsley JM. Biosynthesis and synthetic biology of psychoactive natural products. *Chem Soc Rev* 2021; **50**:6950−7008.
5. Wallwey C, Li SM. Ergot alkaloids: structure diversity, biosynthetic gene clusters and functional proof of biosynthetic genes. *Nat Prod Rep* 2011;**28**:496−510.
6. Liu H, Jia Y. Ergot alkaloids: synthetic approaches to lysergic acid and clavine alkaloids. *Nat Prod Rep* 2017;**34**:411−32.
7. Beaulieu WT, Panaccione DG, Quach QN, Smoot KL, Clay K. Diversification of ergot alkaloids and heritable fungal symbionts in morning glories. *Commun Biol* 2021;**4**:1362.
8. Florea S, Panaccione DG, Schardl CL. Ergot alkaloids of the family Clavicipitaceae. *Phytopathology* 2017;**107**:504−18.
9. Chen JJ, Han MY, Gong T, Yang JL, Zhu P. Recent progress in ergot alkaloid research. *RSC Adv* 2017;**7**:27384−96.
10. Hulvová H, Galuszka P, Frébortová J, Frébort I. Parasitic fungus *Claviceps* as a source for biotechnological production of ergot alkaloids. *Biotechnol Adv* 2013;**31**:79−89.
11. Haarmann T, Rolke Y, Giesbert S, Tudzynski P. Ergot: from witchcraft to biotechnology. *Mol Plant Pathol* 2009;**10**:563−77.
12. Sang M, Feng P, Chi L-P, Zhang W. The biosynthetic logic and enzymatic machinery of approved fungi-derived pharmaceuticals and agricultural biopesticides. *Nat Prod Rep* 2024;**41**:565−603.
13. Sharma N, Sharma VK, Manikyam HK, Krishna AB. Ergot alkaloids: a review on therapeutic applications. *Eur J Med Plants* 2016;**14**:1−17.
14. Reddy P, Vincent D, Hemsworth J, Ezernieks V, Guthridge K, Spangenberg GC, et al. Effects of ergotamine on the central nervous system using untargeted metabolomics analysis in a mouse model. *Sci Rep* 2021;**11**:19542.
15. Silberstein SD, Shrewsbury SB, Hoekman J. Dihydroergotamine (DHE)−then and now: a narrative review. *Headache* 2020;**60**: 40−57.
16. Gurung AB, Ali MA, Lee J, Farah MA, Al-Anazi KM. *In silico* screening of FDA approved drugs reveals ergotamine and dihydroergotamine as potential coronavirus main protease enzyme inhibitors. *Saudi J Biol Sci* 2020;**27**:2674−82.
17. Bergamasco B, Frattola L, Muratorio A, Piccoli F, Mailland F, Parnetti L. α-Dihydroergocryptine in the treatment of *de novo* parkinsonian patients: results of a multicentre, randomized, double-blind, placebo-controlled study. *Acta Neurol Scand* 2000;**101**:372−80.
18. Holt R, Barnett A, Bailey C. Bromocriptine: old drug, new formulation and new indication. *Diabetes Obes Metab* 2010;**12**:1048−57.
19. Hoyer D. Targeting the 5-HT system: potential side effects. *Neuropharmacology* 2020;**179**:108233.
20. Haarmann T, Machado C, Lübbe Y, Correia T, Schardl CL, Panaccione DG, et al. The ergot alkaloid gene cluster in *Claviceps purpurea*: extension of the cluster sequence and intra species evolution. *Phytochemistry* 2005;**66**:1312−20.
21. Jakubczyk D, Cheng JZ, O'Connor SE. Biosynthesis of the ergot alkaloids. *Nat Prod Rep* 2014;**31**:1328−38.
22. Li S-M, Unsöld IA. Post-genome research on the biosynthesis of ergot alkaloids. *Planta Med* 2006;**72**:1117−20.
23. Wu N, Yao M, Xiao W, Dong T, Ma H, Du X, et al. Modular pathway compartmentalization for agroclavine overproduction in *Saccharomyces cerevisiae*. *ACS Synth Biol* 2023;**12**:1133−45.
24. Yu Z-P, An C, Yao Y, Wang C-Y, Sun Z, Cui C, et al. A combined strategy for the overproduction of complex ergot alkaloid agroclavine. *Synth Syst Biotechnol* 2022;**7**:1126−32.
25. Jastrzębski MK, Kaczor AA, Wróbel TM. Methods of lysergic acid synthesis-the key ergot alkaloid. *Molecules* 2022;**27**:7322.
26. Wong G, Lim LR, Tan YQ, Go MK, Bell DJ, Freemont PS, et al. Reconstituting the complete biosynthesis of d-lysergic acid in yeast. *Nat Commun* 2022;**13**:712.
27. Correia T, Grammel N, Ortel I, Keller U, Tudzynski P. Molecular cloning and analysis of the ergopeptine assembly system in the ergot fungus *Claviceps purpurea*. *Chem Biol* 2003;**10**:1281−92.
28. Riederer B, Han M, Keller U. D-Lysergyl peptide synthetase from the ergot fungus *Claviceps purpurea*. *J Biol Chem* 1996;**271**:27524−30.
29. Zhang L, Wang C, Chen K, Zhong W, Xu Y, Molnár I. Engineering the biosynthesis of fungal nonribosomal peptides. *Nat Prod Rep* 2023;**40**: 62−88.
30. Marahiel MA. A structural model for multimodular NRPS assembly lines. *Nat Prod Rep* 2016;**33**:136−40.
31. Ortel I, Keller U. Combinatorial assembly of simple and complex d-lysergic acid alkaloid peptide classes in the ergot fungus *Claviceps purpurea*. *J Biol Chem* 2009;**284**:6650−60.
32. Havemann J, Vogel D, Loll B, Keller U. Cyclolization of d-lysergic acid alkaloid peptides. *Chem Biol* 2014;**21**:146−55.
33. Lorenz N, Haarmann T, Pažoutová S, Jung M, Tudzynski P. The ergot alkaloid gene cluster: functional analyses and evolutionary aspects. *Phytochemistry* 2009;**70**:1822−32.
34. Lorenz N, Wilson EV, Machado C, Schardl CL, Tudzynski P. Comparison of ergot alkaloid biosynthesis gene clusters in *Claviceps* species indicates loss of late pathway steps in evolution of *C. fusiformis*. *Appl Environ Microbiol* 2007;**73**:7185−91.
35. Haarmann T, Lorenz N, Tudzynski P. Use of a nonhomologous end joining deficient strain (*Δku70*) of the ergot fungus *Claviceps purpurea* for identification of a nonribosomal peptide synthetase gene involved in ergotamine biosynthesis. *Fungal Genet Biol* 2008;**45**:35−44.
36. Chen JJ, Han MY, Gong T, Qiao YM, Yang JL, Zhu P. Epigenetic modification enhances ergot alkaloid production of *Claviceps purpurea*. *Biotechnol Lett* 2019;**41**:1439−49.
37. Miličić S, Kremser M, Gaberc-Porekar V, Didek-Brumec M, Sočić H. The effect of aeration and agitation on *Claviceps purpurea*

dimorphism and alkaloid synthesis during submerged fermentation. *Appl Microbiol Biotechnol* 1989;**31**:134−7.
38. Yao Y, Wang W, Shi W, Yan R, Zhang J, Wei G, et al. Overproduction of medicinal ergot alkaloids based on a fungal platform. *Metab Eng* 2022;**69**:198−208.
39. Qiao YM, Wen YH, Gong T, Chen JJ, Chen TJ, Yang JL, et al. Improving ergometrine production by *easO* and *easP* knockout in *Claviceps paspali*. *Fermentation* 2022;**8**:263.
40. Yin WB, Chooi YH, Smith AR, Cacho RA, Hu Y, White TC, et al. Discovery of cryptic polyketide metabolites from dermatophytes using heterologous expression in *Aspergillus nidulans*. *ACS Synth Biol* 2013; **2**:629−34.
41. Szewczyk E, Nayak T, Oakley CE, Edgerton H, Xiong Y, Taheri-Talesh N, et al. Fusion PCR and gene targeting in *Aspergillus nidulans*. *Nat Protoc* 2006;**1**:3111−20.
42. Schwede T, Kopp J, Guex N, Peitsch MC. SWISS-MODEL: an automated protein homology-modeling server. *Nucleic Acids Res* 2003;**31**: 3381−5.
43. Chiang YM, Ahuja M, Oakley CE, Entwistle R, Asokan A, Zutz C, et al. Development of genetic dereplication strains in *Aspergillus nidulans* results in the discovery of aspercryptin. *Angew Chem Int Ed* 2016;**55**:1662−5.
44. Chiang Y-M, Oakley CE, Ahuja M, Entwistle R, Schultz A, Chang SL, et al. An efficient system for heterologous expression of secondary metabolite genes in *Aspergillus nidulans*. *J Am Chem Soc* 2013;**135**: 7720−31.
45. Ryan KL, Moore CT, Panaccione DG. Partial reconstruction of the ergot alkaloid pathway by heterologous gene expression in *Aspergillus nidulans*. *Toxins* 2013;**5**:445−55.
46. Huang T, Li L, Brock NL, Deng Z, Lin S. Functional characterization of PyrG, an unusual nonribosomal peptide synthetase module from the pyridomycin biosynthetic pathway. *Chembiochem* 2016;**17**:1421−5.
47. Challis GL, Ravel J, Townsend CA. Predictive, structure-based model of amino acid recognition by nonribosomal peptide synthetase adenylation domains. *Chem Biol* 2000;**7**:211−24.
48. Yan DJ, Chen QB, Gao J, Bai J, Liu BY, Zhang YL, et al. Complexity and diversity generation in the biosynthesis of fumiquinazoline-related peptidyl alkaloids. *Org Lett* 2019;**21**:1475−9.
49. Leuchtmann A, Bacon CW, Schardl CL, White Jr JF, Tadych M. Nomenclatural realignment of *Neotyphodium* species with genus Epichloë. *Mycologia* 2014;**106**:202−15.
50. Kalb D, Lackner G, Hoffmeister D. Fungal peptide synthetases: an update on functions and specificity signatures. *Fungal Biol Rev* 2013;**27**: 43−50.